

Article

# A Computational Study of Metallacycles Formed by Pyrazolate Ligands and the Coinage Metals M = Cu(I), Ag(I) and Au(I): (pzM)<sub>n</sub> for n = 2, 3, 4, 5 and 6. Comparison with Structures Reported in the Cambridge Crystallographic Data Center (CCDC)

José Elguero and Ibon Alkorta \* 

Instituto de Química Médica (IQM-CSIC), Juan de la Cierva, 3, E-28006 Madrid, Spain; iqmbe17@iqm.csic.es

\* Correspondence: ibon@iqm.csic.es; Tel.: +34-915622900

Academic Editors: Vera L. M. Silva and Artur M. S. Silva

Received: 30 September 2020; Accepted: 21 October 2020; Published: 3 November 2020



**Abstract:** The structures reported in the Cambridge Structural Database (CSD) for neutral metallacycles formed by coinage metals in their valence (I) (cations) and pyrazolate anions were examined. Depending on the metal, dimers and trimers are the most common but some larger rings have also been reported, although some of the larger structures are not devoid of ambiguity. M06-2x calculations were carried out on simplified structures (without C-substituents on the pyrazolate rings) in order to facilitate a comparison with the reported X-ray structures (geometries and energies). The problems of stability of the different ring sizes were also analyzed.

**Keywords:** X-ray; pyrazolate; coinage metals; metallacycles; M06-2x

## 1. Introduction

There is a field in organometallic chemistry that has rightly demanded a great deal of attention, namely, the cyclic complexes between coinage metal cations and anionic pyrazolate ligands [1]. These metallacycles frequently have high symmetry and contain several nuclei with spin  $I = 1/2$ , which makes them ideally suited for NMR studies:  $^1\text{H}$ ,  $^{13}\text{C}$ ,  $^{15}\text{N}$ ,  $^{19}\text{F}$  (from the much studied 3,5-bis-trifluoromethylpyrazole) and  $^{107/109}\text{Ag}$ . In contrast,  $^{63/65}\text{Cu}$  and  $^{197}\text{Au}$  are quadrupolar ( $I = 3/2$ ) and have therefore been explored to a much lesser extent.

It is common in publications in the field of coordination compounds that single-crystal X-ray structures are reported. In such cases the data are in the Results and Supporting Information sections. Note that there are some publications that concern other aspects of these compounds such as their use in sensors, optical properties, and theoretical calculations where crystal structures are not reported. Earlier papers should also be mentioned here because, although they do not contain crystal structures, they were key in generating interest in these metallacycles [2–4]. Lintang et al. reported that trinuclear group 11 metal pyrazolate complexes are phosphorescent chemosensors for the detection of benzene [5] (for two recent papers on photoluminescence of the Dias and Fujisawa groups see [6,7]). The Serrano group published several papers that describe compounds related to those discussed in the present paper but with interesting mesogen properties when the pyrazolate ligands have long chains in positions three and five and the metal is Cu, Ag or Au [8–11]. Cano's group published similar results for complexes with gold(I) [12].

Of particular relevance is a theoretical paper concerning the study of group 11 pyrazolate complexes. In this case, Caramori, Frenking et al. [13] discussed the trinuclear (pzM)<sub>3</sub> complexes (M = Cu(I), Ag(I) and Au(I)) in terms of different approaches including energy decomposition analysis

(EDA), natural bond orbital (NBO) and anisotropy of the induced current density (ACID). The main conclusions were that the pz-M bond has an elevated covalent character, especially when  $M = \text{Au(I)}$ , and that the pyrazole ligands are strongly aromatic, although they are insulated because there is no through-bond metal-ligand conjugation.

Our group published a paper, in collaboration with Rasika Dias and another with Kiyoshi Fujisawa, on the NMR study of the organometallic nine-membered rings corresponding to trinuclear silver(I) complexes of pyrazolate ligands [14,15], and another on regium bonds between dinuclear silver(I) pyrazolates complexes and Lewis bases [16], two on regium bonds formed by  $\text{Au}_2$  [17] and  $\text{Ag}_2$ ,  $\text{Cu}_2$  and mixed binary regium molecules [18], and finally, one on the comparison of acidity of  $\text{Au(I)}$  and  $\text{Au(III)}$  [19].

## 2. Results and Discussion

The present publication is divided into three sections. The first section concerns an exploration of the Cambridge Structural Database (CSD) [20] in a search for the structures of pyrazolates with coinage metals of valence (I): i.e.,  $\text{Cu(I)}$ ,  $\text{Ag(I)}$  and  $\text{Au(I)}$ ; they will be reported using their refcodes. The second section covers a theoretical study of the stability of these metallacycles as a function of the ring size (dimers, trimers, tetramers, pentamers and hexamers) using the pyrazole itself as a model, i.e., without C-substituents and without supplementary ligands on the metals. The final section concerns the analysis of some metallacycles by Bader's quantum theory of atoms in molecules methodology (QTAIM) [21–24].

We will start with the exploration of the CSD [20]; this search was similar to one carried out by us on the cyclamers formed by NH-pyrazoles based on hydrogen bonds (HBs). NH-pyrazoles crystallize as catemers (chains) and cyclamers (rings with  $n$  pyrazoles), with examples reported for  $n = 2, 3, 4$ , and 6 (rare) but none for a pentamer [25,26] (Figure 1).

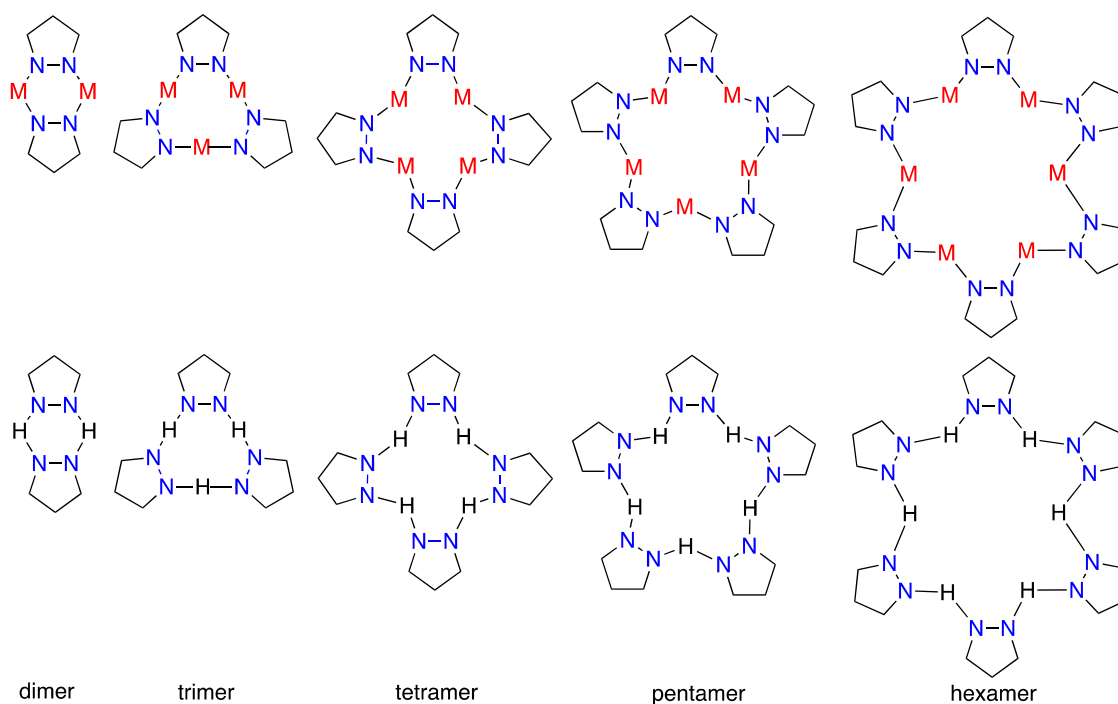


**Figure 1.** Metallacycles (**top**) and the corresponding cyclamers (**bottom**).

### 2.1. Analysis of the Reported CSD Structures (Hits) and Their Refcodes

Before discussing the most relevant hits, it is worth noting that there is only one compound that contains two different metals ( $\text{Ag}_2\text{Au}$ ), namely a gold(I)imidazolate-silver(I)pyrazolate complex, MAMQIB [27] and MAMQIB01 [28] (Figure 2), but this only has two pyrazolates, with the third ligand

being an carbeniate (C,N ligand). In any case, this example shows that  $[pzM(M')]_n$  compounds should be possible with different metals, although examples have not been reported to date.

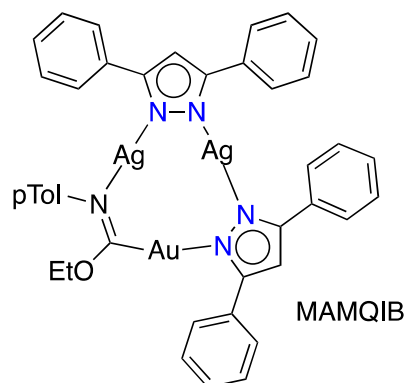


**Figure 2.** Structure of CSD Refcode MAMQIB.

### 2.1.1. Copper, Only Cu(I) Structures (Cu(II) Structures Were Excluded)

Dimers and trimers,  $(pzCu)_2$  and  $(pzCu)_3$ , are common. As far as dimers are concerned, many of these are Cu(II) derivatives and all examples that contain Cu(I) have complex pyrazolates with arms that are able to coordinate the copper or they have supplementary ligands; dimers in which the Cu(I) atoms are “nude”, i.e., linked only to the pyrazolate anion, have not been found. Amongst the supplementary ligands are CO (COCZAY [29], COCZOM [29]),  $C\equiv N-R$  (GITJUO [30], HEDFIF [31], JEMCAF [32]),  $PPh_3$  (GITKEZ [30], PIRDAY [33], SATKAC [34]), pyridines (IPIGET [35], KUKLOR [36]) and *N*-heterocyclic carbenes NHCs (NETLUW [37], NETMAD [37]). The central metallacycle can adopt planar or folded conformations, either boat-type or chair-type (Figure 3), and both of these conformations are common. An examination of the Cu...Cu distances in  $(pzCu)_2$  structures gave 320 values, with a mean value of 3.719 Å, a minimum of 3.013 Å (UTEWUM [38]) and a maximum of 4.074 Å (YADVEG [39]) (Figure 3).

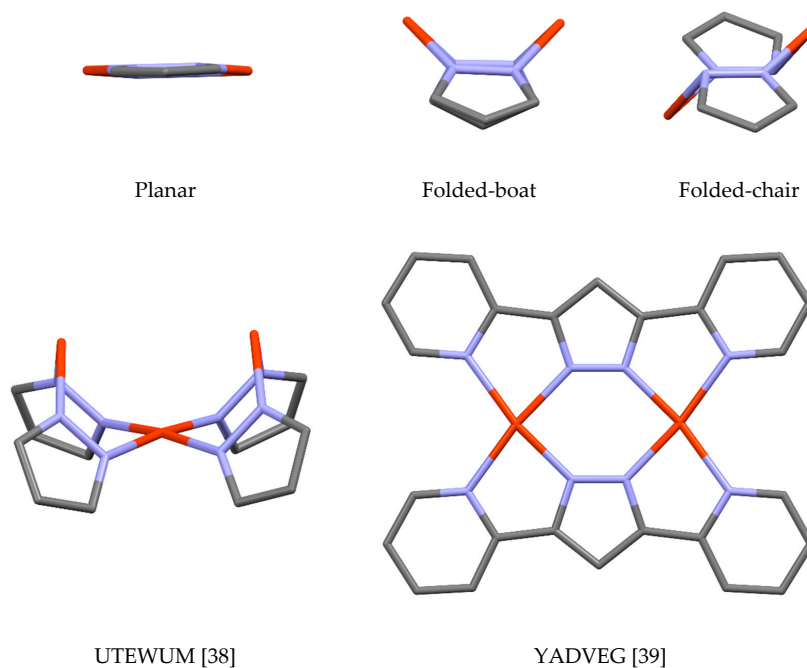


**Figure 3.** Planar and folded conformations of the metallacycle in  $(pzCu)_2$  (simplified representations of UTEWUM and YADVEG).

As far as trimers are concerned, the two main classes are isolated trimers and double trimers and we proposed to denote the latter as “3 + 3”. The simplest derivatives of isolated trimers include CODBAB (4-Cl-pyrazolate) [40], VIJMUW (3,5-diMe-pyrazolate) [41], BELTOC (3,5-di-*i*-Pr-pyrazolate) [42] and XELXAN (3,5-di-CF<sub>3</sub>-pyrazolate) [43].

Simple examples of “3 + 3” double trimers (Figure 4) are IDUYOW (3-Ph-pyrazolate) [44], TANRUW (3-CF<sub>3</sub>-pyrazolate) [32] and GITJIC (3,5-diMe-4-NO<sub>2</sub>-pyrazolate) [30] with near one bond between the triangles formed by Cu atoms and XOGJOU (4-NO<sub>2</sub>-pyrazolate) [45] with near three Cu-Cu bonds. The superimposed structures of double trimers can be a perfect fit, e.g., XOGJOU [45] or rotated (an example will be discussed later for another metal).

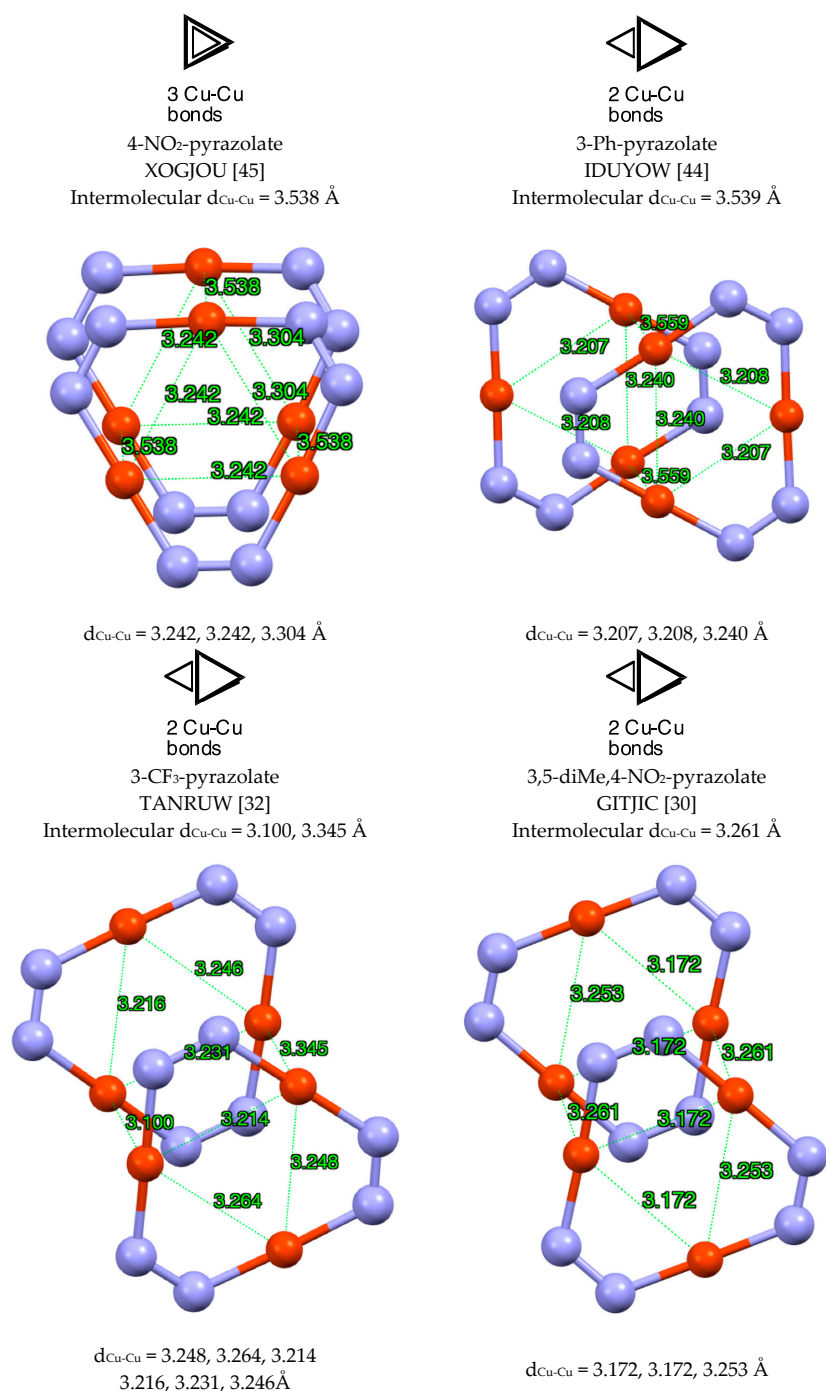


**Figure 4.** Different modes present in the “3 + 3” (pzCu)<sub>3</sub> complexes. Only the copper and nitrogen atoms are represented.

Tetramers (pzCu)<sub>4</sub> are frequently observed and the simplest derivatives include BELTUI [42] (and BELTUI01 [46]), HEDFEB [31], (and OMIPOP01 [42]), OMIPOP [47] and REWWOI [48] (Figure 5). Most Cu<sub>4</sub> rings are planar but in REWWOI [48] this ring is not planar. The structure of OMIPOP [42] was represented with two Cu atoms bonded to both N atoms of the corresponding pyrazolate but this is only the result of a CSD convention that bonds are depicted when they are shorter than the sum of the van der Waals radii. In the original article [48] it is highlighted that the four Cu atoms form a rhombus with a Cu...Cu non-bonding interaction for the shortest distance corresponding to d<sup>10</sup>-d<sup>10</sup> contacts. Fujisawa re-examined this interesting structure (OMIPOO01 [42] and OMIPOO02 [46]) and noted the diamond-like disposition of the four Cu atoms with a short (3.40 Å) and a long (4.85 Å) structure.

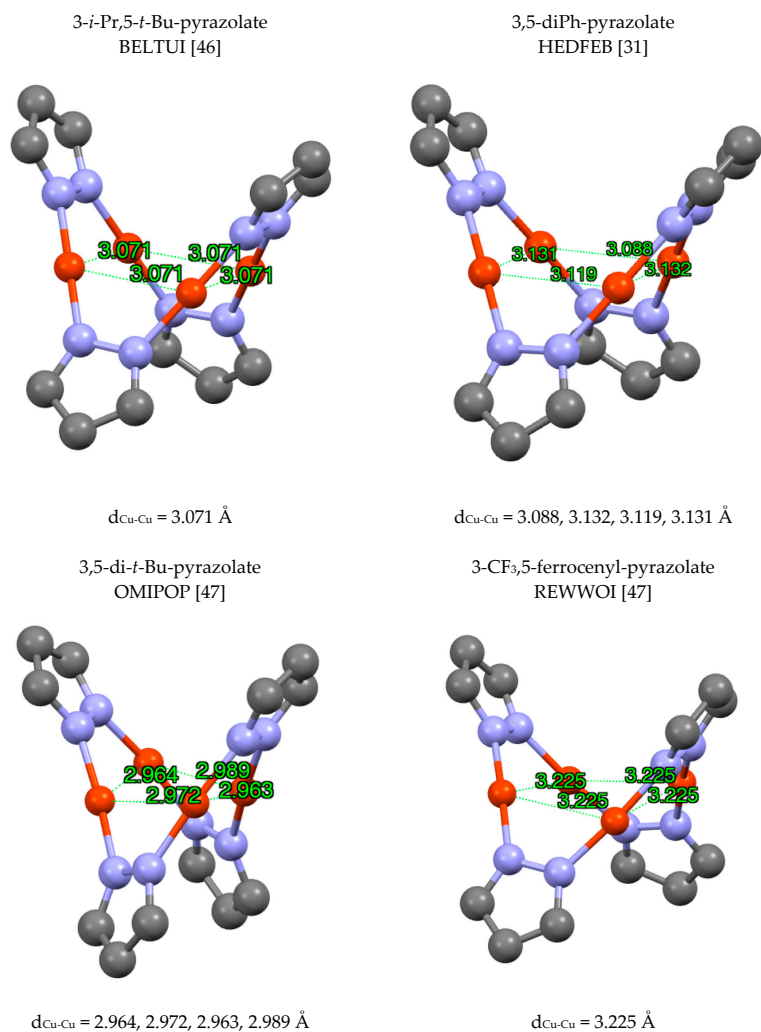


**Figure 5.** Different modes of (pzCu)<sub>4</sub> complexes. Only the copper atoms and the pyrazolate rings are represented. The sequential Cu-Cu distances are listed.

At this point it is worth commenting on hexamers, (pzCu)<sub>6</sub>; these structures always contain six central OH bridges to form a star of alternated Cu atom and O atoms, which means that these are Cu(II) derivatives (QIMWOA and QIMWUG (Coronado et al. [49]) and SASXIW (Galassi, Martins et al. [34])). In summary, examples of Cu(I) pentamers or hexamers are not known.

### 2.1.2. Silver, Only Ag(I) Derivatives

Compounds with (pzAg)<sub>2</sub> and (pzAg)<sub>3</sub> structures are common. As in the case of (pzCu)<sub>2</sub>, in (pzAg)<sub>2</sub> the hexagonal metallacycle adopts planar and folded conformations, with the latter being either boat-like

(the most common) or chair-like (as in cyclohexane), with the silver atoms located at the tips. The mean value of the Ag...Ag distance is 3.755 Å (shortest 3.425 Å, longest 4.305 Å).

Three topological dispositions of double trimers "3 + 3" were found in the CSD (Figure 6), namely three common sides, one common side and one common vertex. These structures are schematically represented in Figure 6 with triangles. These dispositions are illustrated with one or two examples for each situation: XOGJUA [45], DAZGIV [50], FISDIV01 [51] and DOJCUC [52] (EWEHAP [53] is similar with an intermolecular distance between silver metal centers of 3.179 Å). The intermolecular Ag...Ag distance decreases with the number of bonds (3.509 Å (three), 3.205 Å (two) and 2.986 Å (one)) and this is probably due to angular strain.

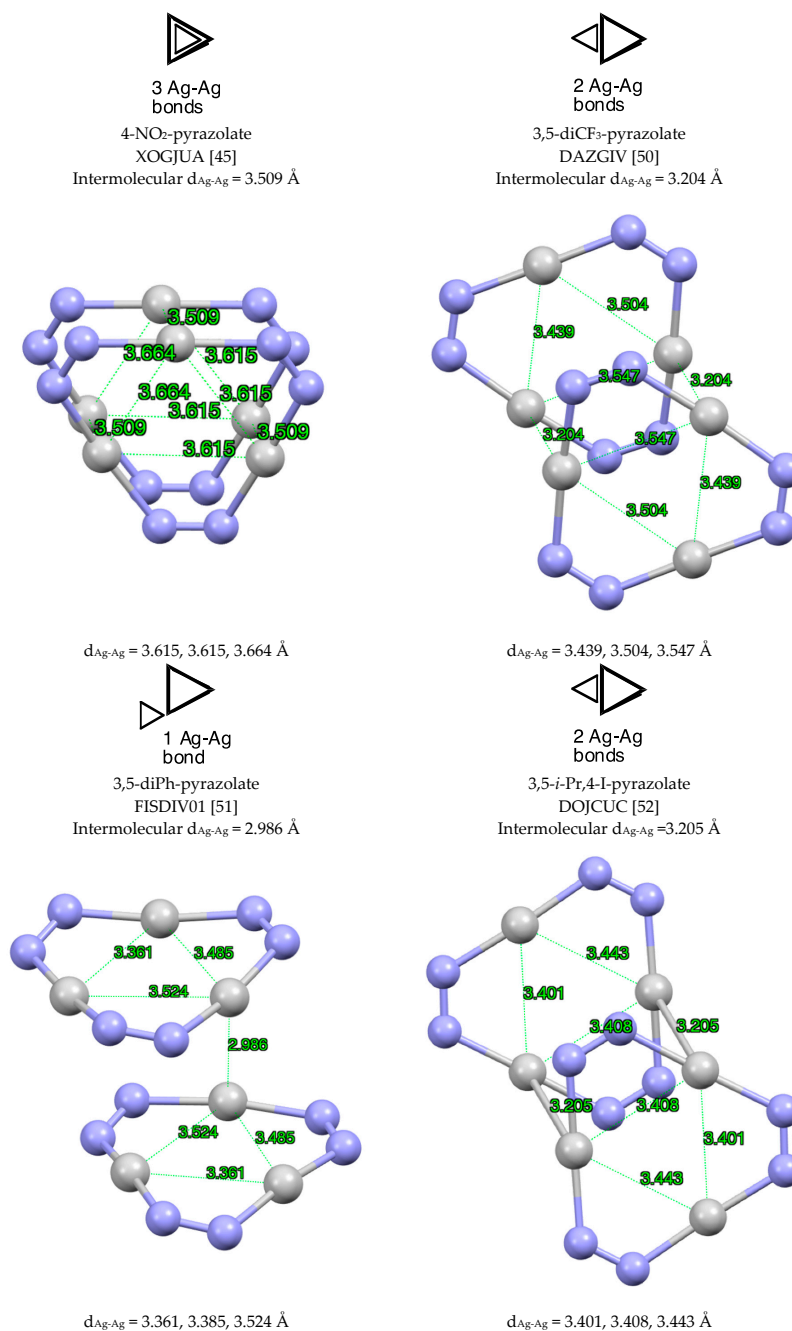


**Figure 6.** Different modes of "3 + 3" (pzAg)<sub>3</sub> complexes. Only the silver and nitrogen atoms are represented.

Tetramers (pzAg)<sub>4</sub> are frequent and, in this case, the simplest structures correspond to GAFJII [46], QEJJOH [54], QEZHEJ [55] and VUPGET [56] (Figure 7).

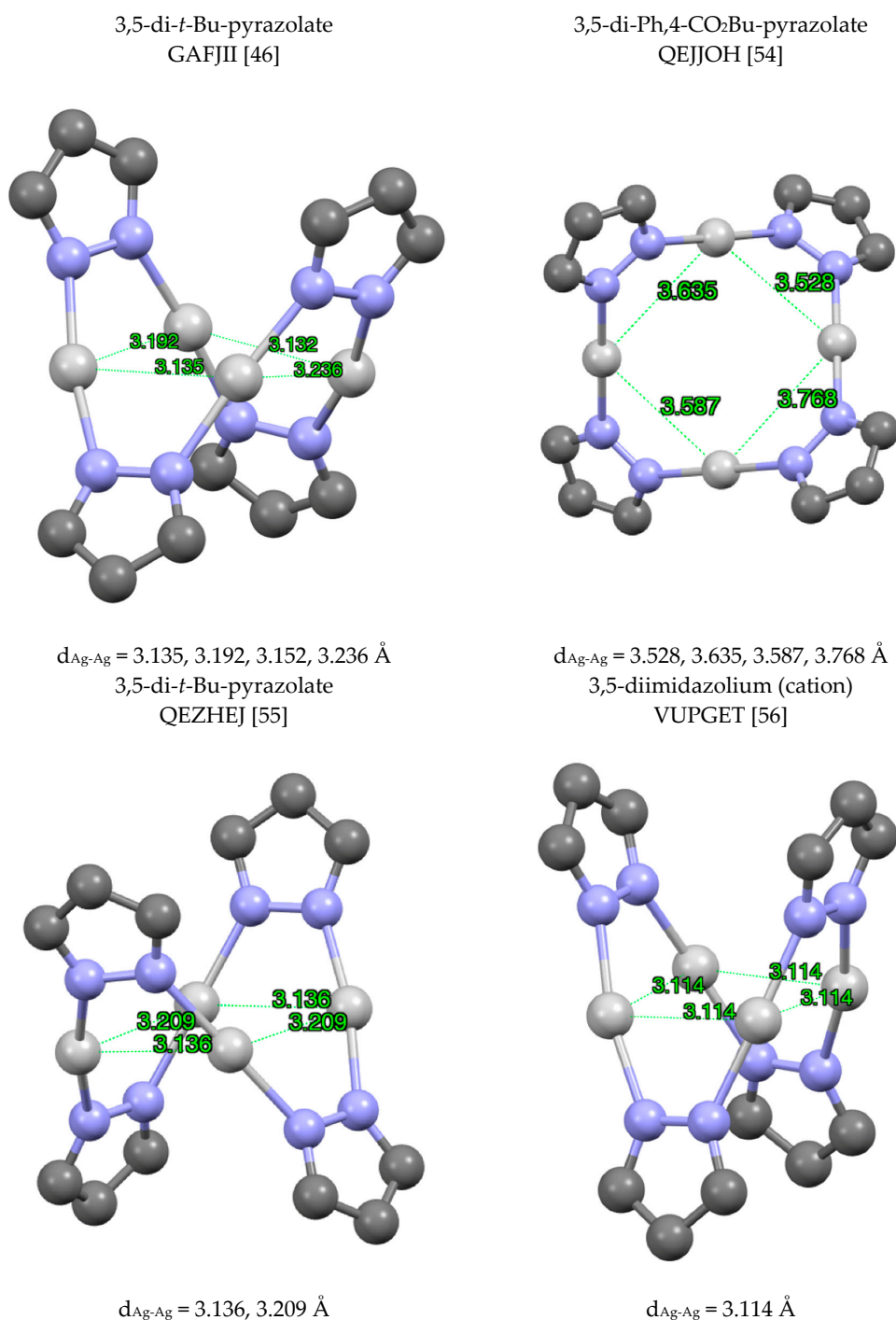


**Figure 7.** Different structures of  $(\text{pzAg})_4$  complexes. Only the silver atoms and the pyrazolate rings are represented. The four examples are very similar but different views have been used.

The structure of SOJCUS [57] is rather complex (Figure 8) in that the silver atoms are double-, triple- and quadruple-coordinated, thus allowing a structure that contains six pyrazolates and five silver atoms. Depending on the itinerary four,  $(\text{pzAg})_4$ , and five,  $(\text{pzAg})_5$ , complexes are present (Figure 8), but a true tetramer or pentamer does not exist.

3,5-di-CF<sub>3</sub>-pyrazolate  
SOJCUS [57]

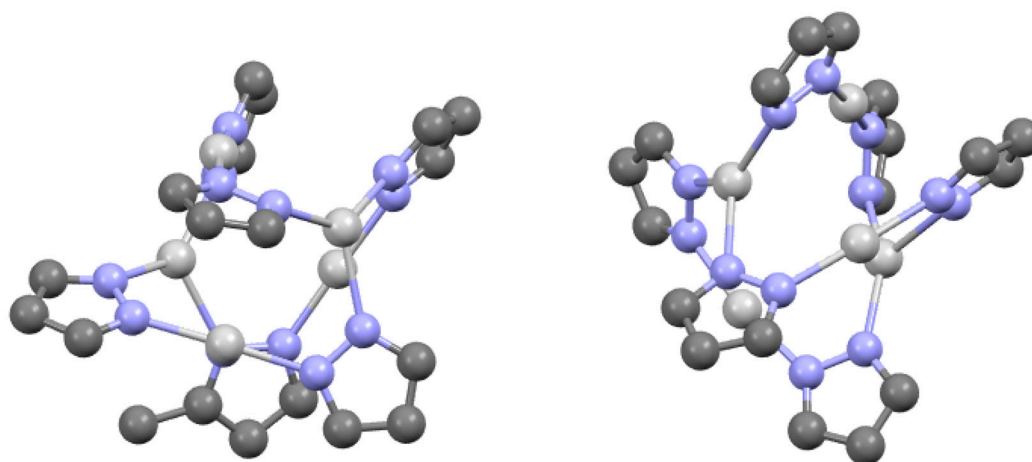


**Figure 8.** A view of the two independent molecules of SOJCUS. Only the silver atoms and the pyrazolate rings are represented.

The only examples of hexamers are QEJJEX [54] and QEJJIB [54] (almost identical), which are beautiful structures that form a loop with short Ag...Ag contacts (QEJJEX [54], Figure 9).

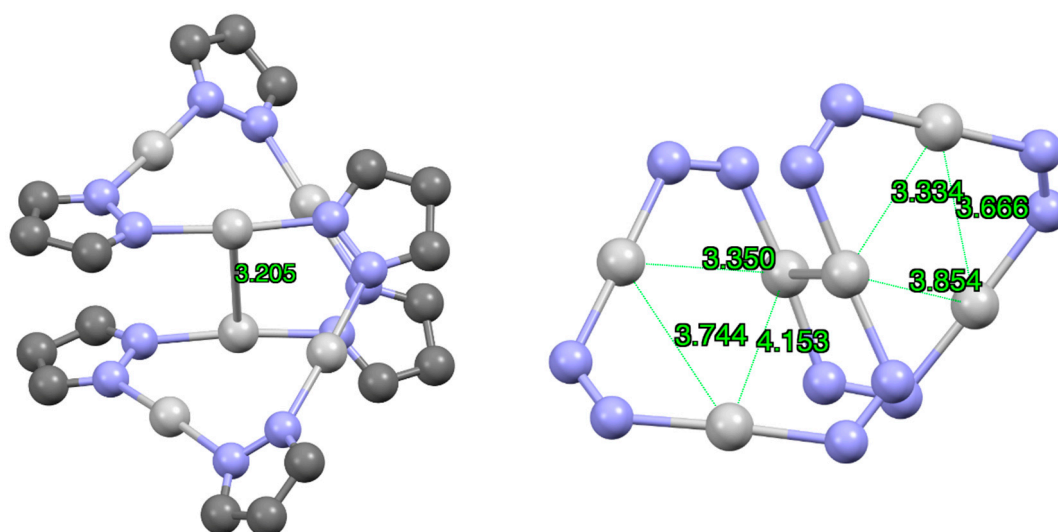


**Figure 9.** Two views of QEJJEX. Only the silver atoms and the pyrazolate rings are represented. Left Ag...Ag distance between loops; right Ag...Ag distance in the quasi-triangles.

In the case of silver, the numbers of structures found in the CSD search were 72 trimers, 16 dimers, 6 tetramers and 2 hexamers (2.1%) (pentamers were not found).

### 2.1.3. Gold, Only Au(I) Structures (Au(III) Structures Were Excluded)

Dimers (pzAu)<sub>2</sub> with Au(I) are not known and all of the examples found in the CSD are Au(III) derivatives. Trimers (pzAu)<sub>3</sub> are common, with some compounds isolated as trimers, e.g., the bis-3,5-CF<sub>3</sub>-pyrazolate, COHFIO01 [50] ( $d_{\text{Au-Au}} = 3.341, 3.350, 3.360 \text{ \AA}$ ) and bis-3,5-Ph-pyrazolate FUWXOK01 [58] ( $d_{\text{Au-Au}} = 3.361 \text{ \AA}$ , a regular triangle) while others (Figure 10) are “3 + 3” double trimers.



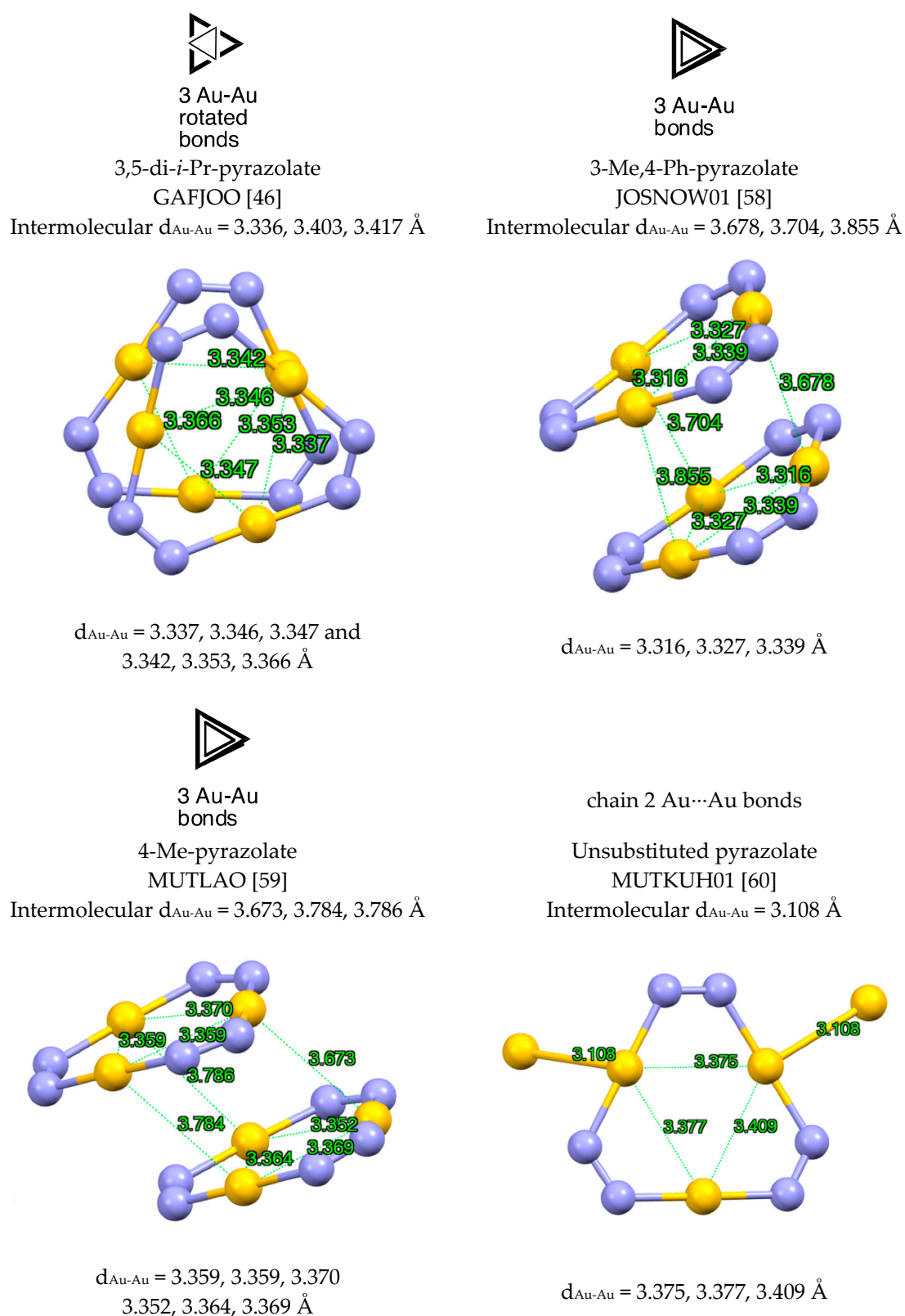


**Figure 10.** Different modes of  $(\text{pzAu})_3$  “3 + 3” complexes. Only the gold and nitrogen atoms are represented [59,60].

Au(I) tetramers, (pzAu)<sub>4</sub>, are known and the simplest examples are GAFJUU [46], GAFKAB [46], OKALER [61] and OKALIV [61] (Figure 11). The gold centers can arrange in a regular square (GAFJUU [46]), in a rectangle (OKALER [61]), in a quadrilateral (GAFKAB [46]) or in a folded quadrilateral (OKALIV [61]).

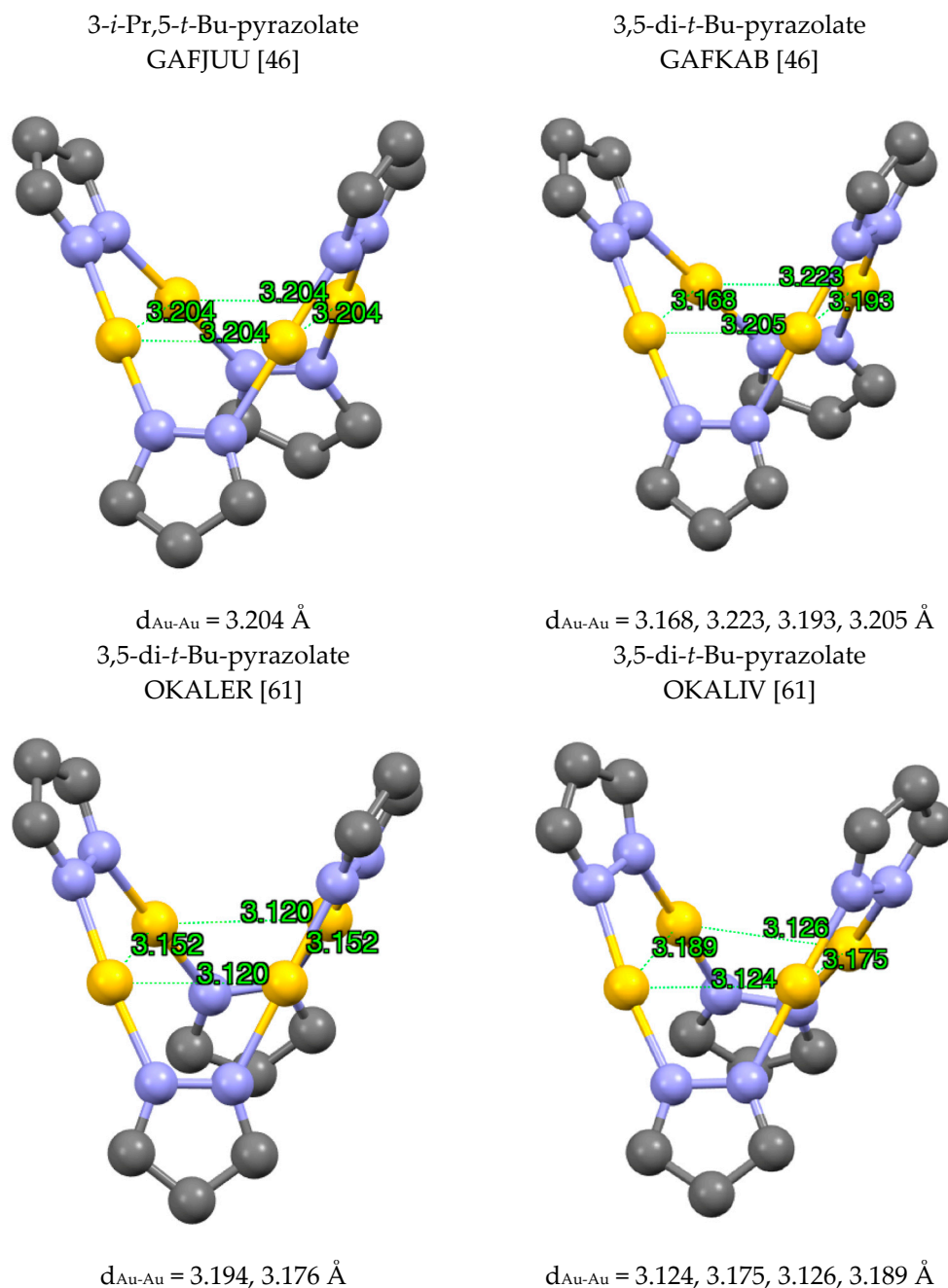


**Figure 11.** Different modes of (pzAu)<sub>4</sub> complexes. Only the gold atoms and the pyrazolate rings are represented.

Finally (pzAu)<sub>6</sub> structures are very rare: in 1988 Raptis reported FEJJA10 [62], see Figure 12.

3,5-diPh-pyrazolate  
FEJJA10 [62]

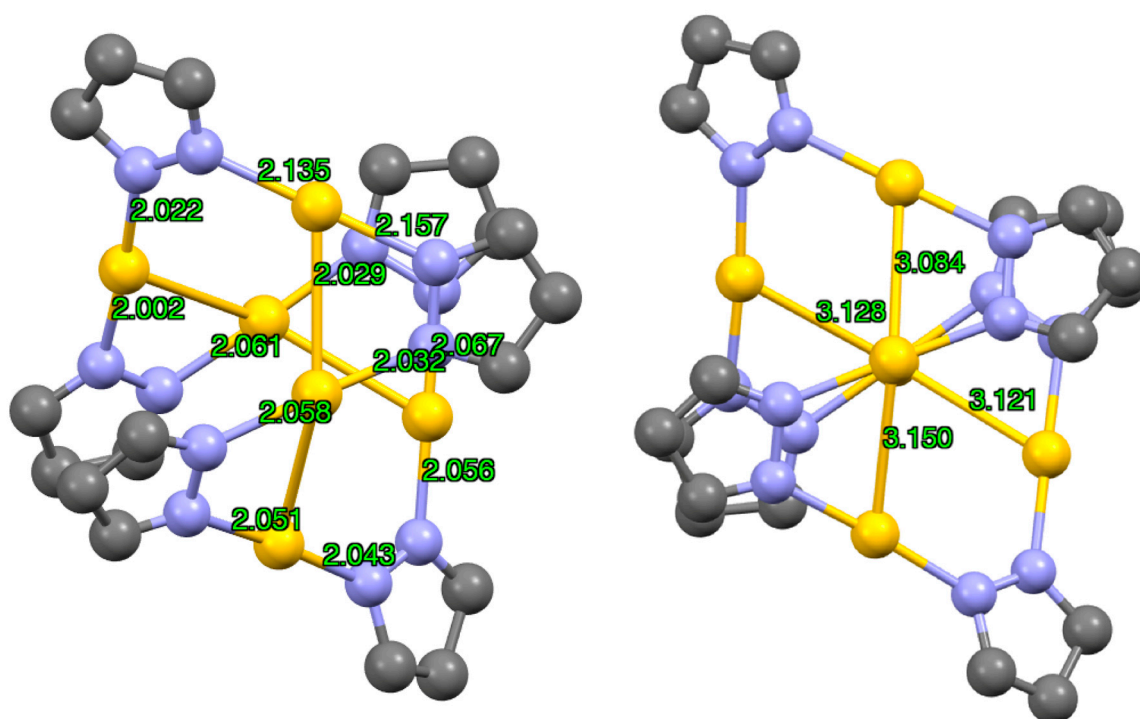


**Figure 12.** Two views of one of the two independent molecules of FEJJA10 with Au-N distances (**left**) and Au-Au distances in Å (**right**). Only the gold atoms and the pyrazolate rings are represented.

On examining the structures of gold(I) reported in the CSD we found 28 trimers, 8 tetramers and 1 hexamer (dimers and pentamers were not found).

The X-ray structures previously discussed are summarized in Table 1 together with NH-pyrazole cyclamers.

**Table 1.** Structures found in the Cambridge Structural Database (CSD) for metallacycles formed by pyrazolate ligands and the coinage metals  $M = \text{Cu(I)}$ ,  $\text{Ag(I)}$  and  $\text{Au(I)}$ :  $(\text{pzM})_n$  for  $n = 2, 3, 4, 5$  and  $6$ . The percentages are in brackets. For comparative purposes, the results for NH-pyrazoles (cyclamers) are also provided. The relative order from frequent to zero (pentamers) is in bold.

Metal/H	Total	Dimers	Trimers	Tetramers	Pentamers	Hexamers (Refcodes)
Cu(I)	81	2 22 [27.2]	1 41 [50.6]	3 18 [22.2]	5 0 [0.0]	4 0 [0.0]
Ag(I)	96	2 6 [6.2]	1 72 [75.0]	3 6 [6.2]	5 0 [0.0]	4 2 (QEJJEX [54], QEJJIB [54]) [2.1]
Au(I)	37	4 0 [0.0]	1 28 [75.7]	2 8 [21.6]	5 0 [0.0]	3 1 (FEJJA10 [62] [2.7])
H [26]	38	1 16 [42.1]	3 8 [21.1]	2 13 [34.2]	5 0 [0.0]	4 1 [2.6]

Thus, the situation has some similarities for H and for M in the sense that NH pyrazoles cyclamers with  $n = 2, 3, 4$ , and  $6$  (rare) have been reported but a pentamer (**5**) has not been reported [25,26]. However, while metallacycles trimers are the most common (**1**), in NH-pyrazoles they occupy only the third position (**3**).

## 2.2. Calculated Structures (Minima in All Cases)

### 2.2.1. Geometries

We calculated different dispositions of the metallacycles using the parent pyrazolate ligand as a model, i.e., without any C-substituent. In the case of dimers, all adopt the planar conformation and never the folded conformation found in the CSD (Figure 13 and Table 2).

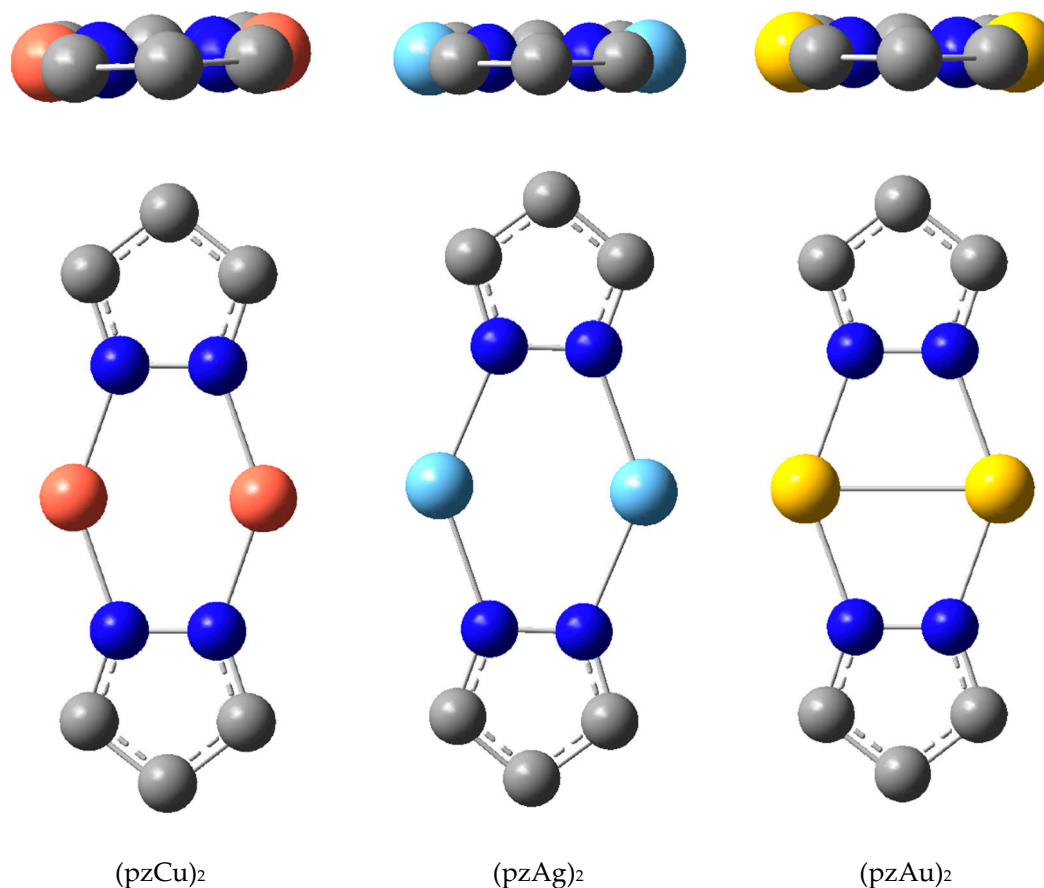


**Figure 13.** Two views of the calculated Cu, Ag and Au dimers; hydrogen atoms have been omitted.

**Table 2.** Calculated mean metal...metal and metal...N atom (Å) (averaged and parent pyrazoles).

Metal	Dimer		Trimer		Tetramer		Hexamer	
	M-M	N-M	M-M	N-M	M-M	N-M	M-M	N-M
Cu(I)	2.656	1.963	3.306	1.921	3.352	1.920	3.447	1.932
Ag(I)	2.953	2.192	3.507	2.124	3.448	2.122	3.631	2.145
Au(I)	2.808	2.124	3.440	2.041	3.478	2.037	3.605	2.042

The trimers lead to triangles and it is interesting to estimate how far they are from the equilateral case that results from a  $D_{3h}$  symmetry in the examples reported in the CSD. The tetramers will lead to squares ( $D_{4h}$ ), planar deformed squares (rectangles, rhombs) and non-planar structures (folded about the M1–M3 edge). The situation increases in complexity as the number of metals increases; for hexamers there are the planar regular hexagon ( $D_{6h}$ ) and several distorted hexagons, including the *ududud* structure (*u* or *d* refers to the *up* or *down* position of the pyrazole ring, as shown schematically in Figure 14).

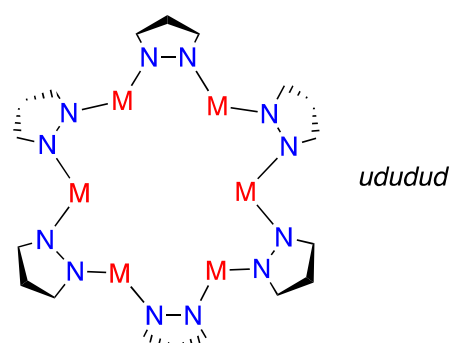
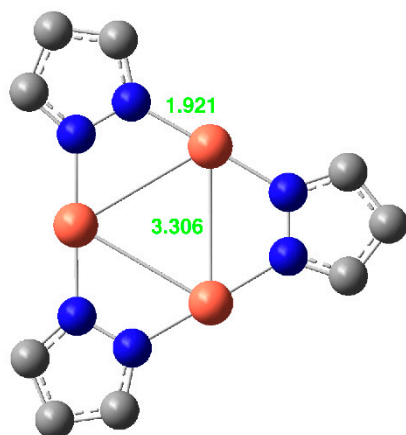


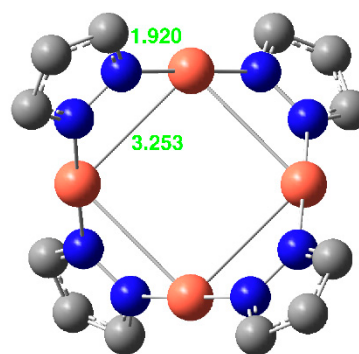
Figure 14. Schematic representation of the *ududud* structure.

We also calculated double dimers (2 + 2) and double trimers (3 + 3) in two orientations. The structures and some distances are represented in the following images for all metallacycles except dimers. The distances that were analyzed are  $M(I)\cdots M(I)$  and  $N\cdots M(I)$ .

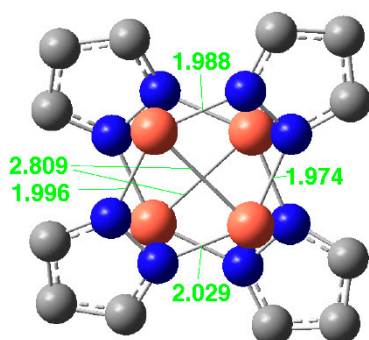
The studied Cu(I) derivatives, beyond monomers and dimers, are represented in Figure 15. The mean distances in the dimers are  $Cu\cdots Cu = 2.656 \text{ \AA}$  and  $N\cdots Cu = 1.963 \text{ \AA}$ .



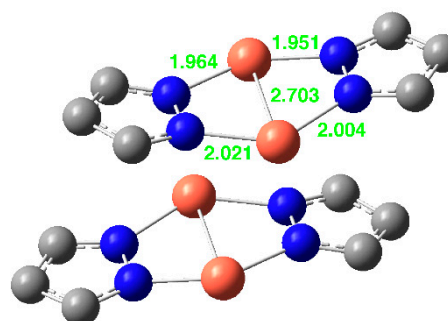
Cu Trimer (regular triangle,  $D_{3h}$ )  
Cu $\cdots$ Cu (3.306 Å) and  
Cu $\cdots$ N distances (1.921 Å)



Cu Tetramer (planar square,  $D_{2d}$ )  
only one Cu $\cdots$ Cu (3.253 Å) and  
one Cu $\cdots$ N distance (1.920 Å)

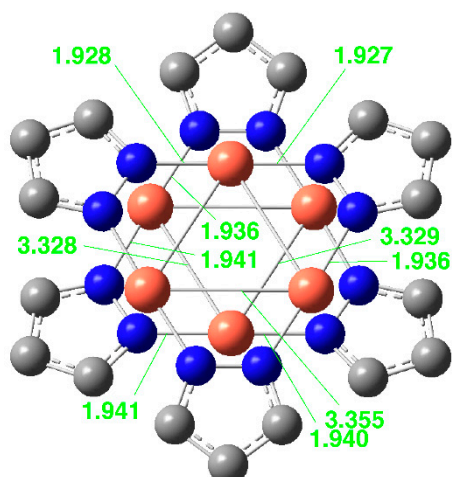


Cu<sub>4</sub> structure: 2 + 2  
Cu $\cdots$ Cu (2.809 Å) and Cu $\cdots$ N  
distances (1.974, 1.987, 1.996, 2.029 Å)

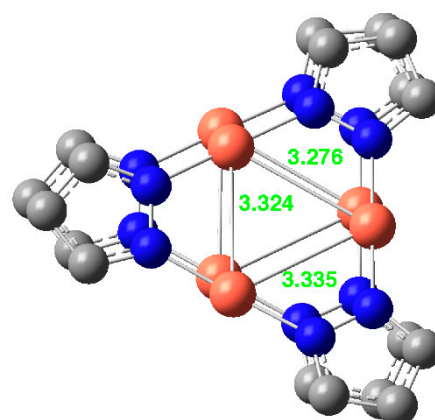


Cu<sub>4</sub>, new structure 2 + 2 (twisted)  
Cu $\cdots$ Cu (2.703 Å) and Cu $\cdots$ N  
distances (1.964, 1.951, 2.004, 2.021 Å)

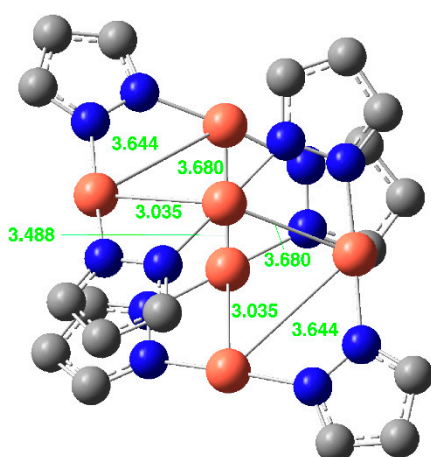
Figure 15. *Cont.*



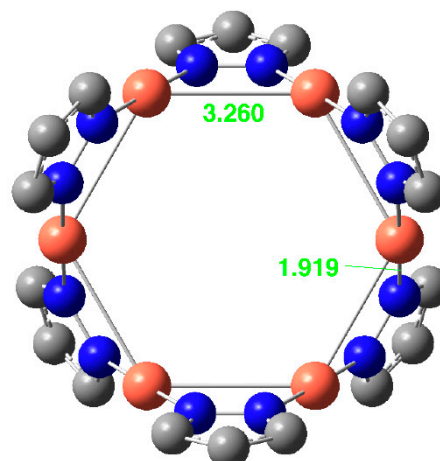
$\text{Cu}_6$  structure: 3 + 3  
 Cu...Cu (3.328, 3.329, 3.355 Å) and  
 Cu...N distances (1.928, 1.928, 1.936, 1.940, 1.940, 1.936  
 Å)



$\text{Cu}_6$ , new structure 3 + 3 (twisted)  
 Cu...Cu (3.276, 3.324, 3.335 Å) and  
 Cu...N distances (1.924, 1.925, 1.929,  
 1.928, 1.937, 1.932 Å)



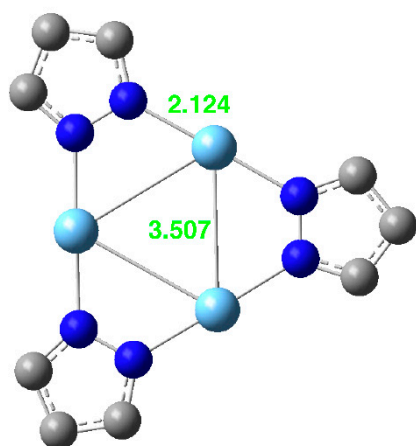
Cu analog of FEJJAF10 hexamer  
 Cu...Cu distances (3.644, 3.680, 3.035, 3.488 and 3.035,  
 3.644 Å)  
 Cu...N distances (1.916, 1.936, 1.944 Å)



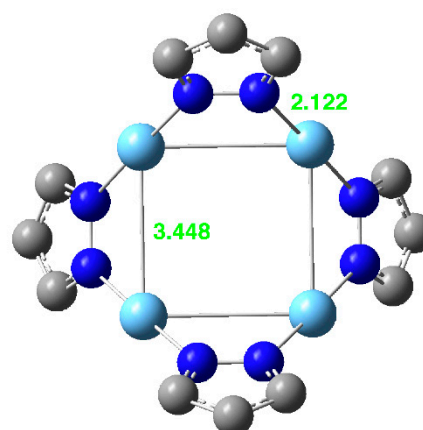
Cu *ududud*  
 Cu...Cu distance 3.260 Å  
 Cu...N distance 1.919 Å

**Figure 15.** Optimized structures of Cu(I) pyrazolates.

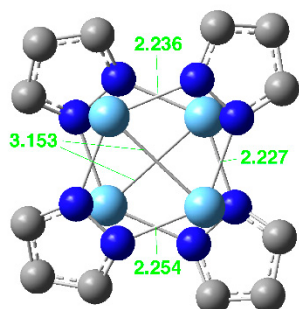
The Ag(I) structures are reported in Figure 16. The average distances for the dimer are Ag...Ag = 2.953 Å and N...Ag = 2.192 Å.



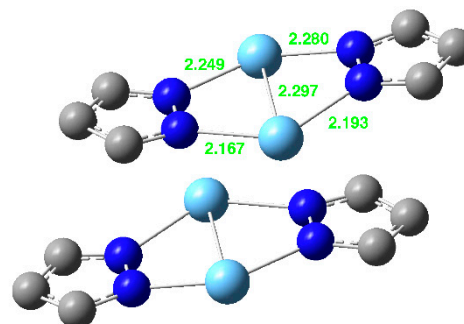
Ag Trimer (regular triangle,  $D_{3h}$ )  
Ag...Ag (3.507 Å) and  
Ag...N distances (2.124 Å)



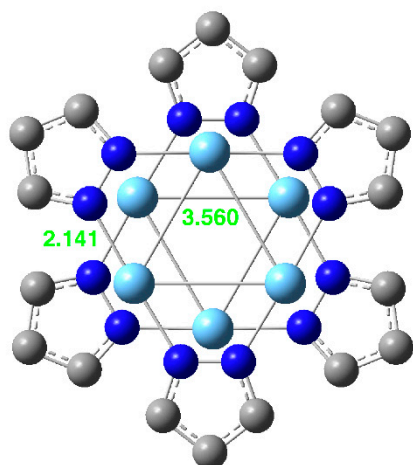
Ag Tetramer (planar square,  $D_{2d}$ )  
only one Ag...Ag (3.448 Å) and  
one Ag...N distance (2.122 Å)



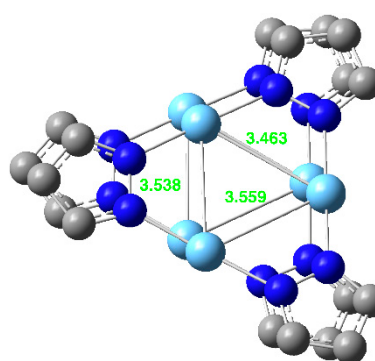
Ag<sub>4</sub> structure: 2 + 2  
Ag...Ag (3.153 Å) and  
Ag...N distances (2.227, 2.236, 2.254 Å)



New 2 + 2 (twisted)  
Ag...Ag (2.997 Å) and  
Ag...N distances (2.167, 2.193, 2.249, 2.280 Å)

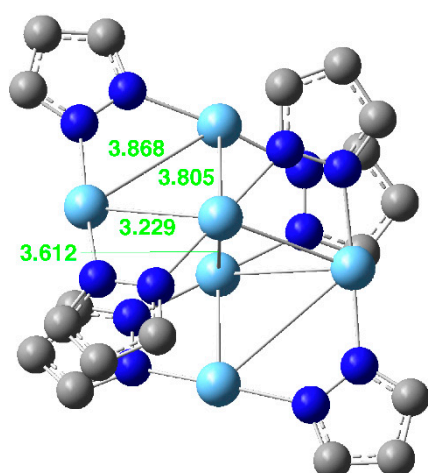


Ag<sub>6</sub> structure: 3 + 3  
Ag...Ag (3.560 Å) and  
Ag...N distances (2.141 Å)

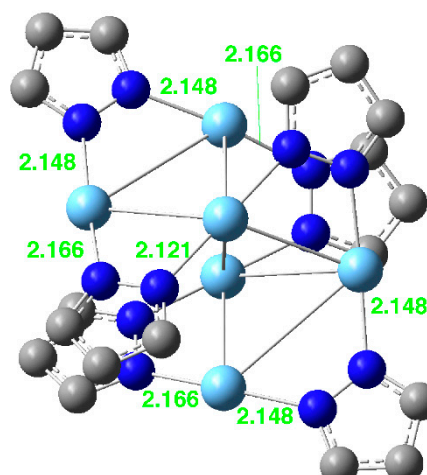


Ag<sub>6</sub>, new structure 3 + 3 (twisted)  
Ag...Ag (3.463, 3.538, 3.559 Å) and  
Ag...N distances (2.126, 2.129, 2.133,  
2.134, 2.153, 2.140 Å)

Figure 16. Cont.



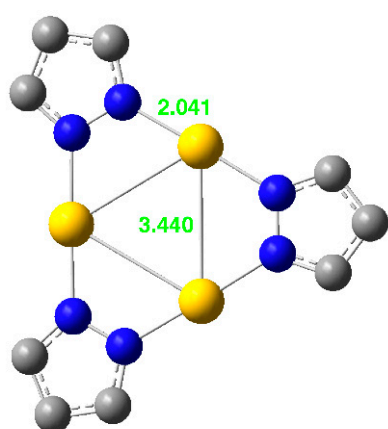
Ag analog of FEJJAF10 hexamer  
Ag...Ag distances (3.229, 3.805, 3.868  
and 3.612 Å)



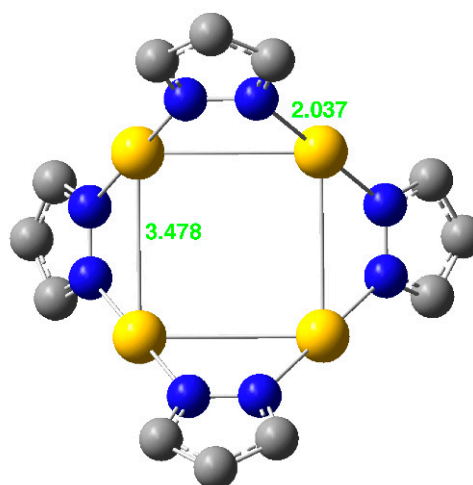
Ag analog of FEJJAF10 hexamer (same structure than on  
the left) Ag...N distances (2.121, 2.148, 2.166 Å)

**Figure 16.** Optimized structures of Ag(I) pyrazolates.

Finally, the studied Au(I) derivatives are represented in Figure 17. For the dimer: Au...Au = 2.808 Å and N...Au = 2.124 Å.



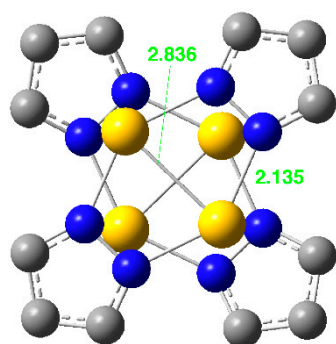
Au Trimer (regular triangle,  $D_{3h}$ )  
Au...Au (3.440 Å) and  
Au...N distances (2.041 Å)



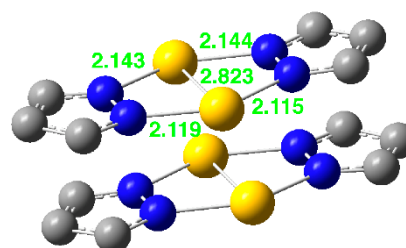
Au Tetramer (planar square,  $D_{2d}$ )  
only one Au...Au (3.478 Å) and  
one Au...N distance (2.037 Å)

**Figure 17.** Cont.

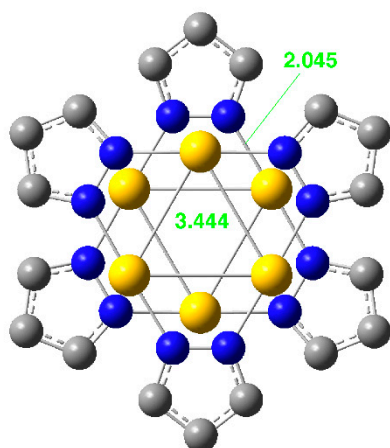




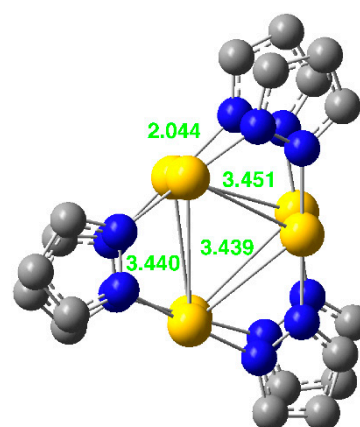
Au<sub>4</sub> structure: 2 + 2  
 Au...Au (2.836 Å) and  
 Au...N distances (2.135 Å)



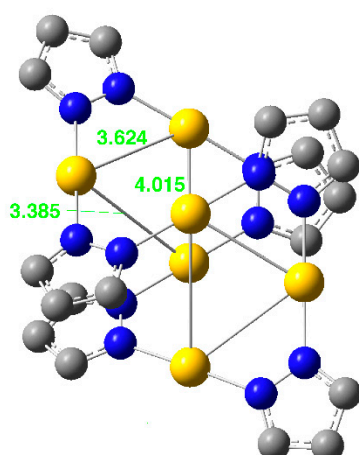
New 2 + 2 (twisted)  
 Au...Au (2.823 Å) and Au...N distances  
 (2.115, 2.119, 2.143, 2.144 Å)



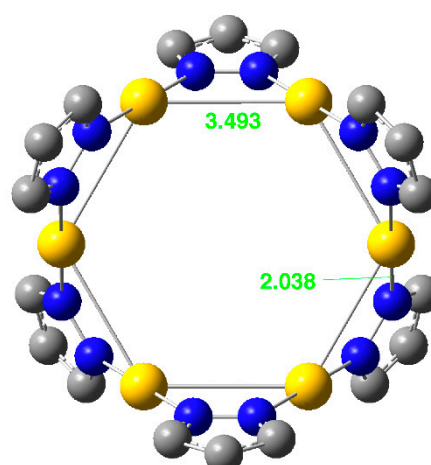
Au<sub>6</sub> structure: 3 + 3  
 Au...Au (3.444 Å) and  
 Au...N distances (2.045 Å)



Au<sub>6</sub>, new structure 3 + 3 (twisted)  
 Au...Au (3.439, 3.440, 3.451 Å) and  
 Au...N distances (2.044 Å)



Au analog of FEJJAF10 hexamer  
 Au...Au distances (3.385, 3.624, 4.015 Å)  
 Au...N distances (2.037, 2.042, 2.046 Å)



Au *ududud* hexamer  
 Au...Au distance 3.493 Å  
 Au...N distance 2.038 Å

Figure 17. Optimized structures of Au(I) pyrazolates.

### 2.2.2. Comparison of Calculated and Measured Geometries (Only Metal...Metal and Metal...Nitrogen Bond Lengths)

The average metal-metal and metal-nitrogen bond lengths in our calculations and in the structures found in the CSD search are gathered in Tables 2–4.

**Table 3.** Measured mean metal...metal and metal...N atom (Å) (averaged and parent pyrazoles).

Metal	Dimer (With Ligands)		Trimer		Tetramer		Hexamer	
	M-M	N-M	M-M	N-M	M-M	N-M	M-M	N-M
Cu(I)	3.424 <sup>a</sup>	1.974 <sup>a</sup>	3.228 <sup>c</sup>	1.858 <sup>c</sup>	3.095 (3)	1.849 (3)	-	-
Ag(I)	3.824 <sup>b</sup>	2.284 <sup>b</sup>	3.520 <sup>d</sup>	2.090 <sup>d</sup>	3.274 (5)	2.073 (5)	3.615 (5)	2.084 (5)
Au(I)	-	-	3.356 <sup>e</sup>	1.994 <sup>e</sup>	3.185 (9)	2.006 (5)	3.121 (10)	2.059 (10)

**Experimental (averaged values)** (the compounds used corresponds to those represented in the corresponding Figures in blue) or to compounds (refcodes) cited in the discussion. Some have been selected to build up this Table. <sup>a</sup> BITSAB [63], IPIGET [35], JEMCAF [32], NETMAD [37]; <sup>b</sup> FINWIL [64], KIRXIV [65], ZIGROŽ [66], ZIGRUF [67]; <sup>c</sup> BELTOC [42], CODBAB [40], VIJMUW [41], XELXAN [43]; <sup>d</sup> AWAWUS [67], CENFIM [68], HICHIL [69], XOGJUA [45]; <sup>e</sup> COHFIO01 [50], FUWXOK01 [58].

**Table 4.** Experimental metal...metal and metal...N atom (Å) (averaged and parent pyrazoles).

Metal	Dimer (With Ligands)		Trimer		Tetramer		Hexamer	
	M-M	N-M	M-M	N-M	M-M	N-M	M-M	N-M
Cu(I)	3.726 <sup>a</sup>	2.010 <sup>a</sup>	3.251 <sup>c</sup>	1.861 <sup>c</sup>	3.394 <sup>f</sup>	1.962 <sup>f</sup>	-	-
Ag(I)	3.788 <sup>b</sup>	2.245 <sup>b</sup>	3.426 <sup>d</sup>	2.200 <sup>d</sup>	None	None	None	None
Au(I)	-	-	3.382 <sup>e</sup>	2.004 <sup>e</sup>	None	None	None	None

**Experimental** (unsubstituted pyrazoles or, at least, only 4-substituted pyrazoles). When neither HHH or HRH pyrazoles were found, none are written in the Table. <sup>a</sup> KIRXOB [65], NETLUW [37]; <sup>b</sup> RATFAT [70], RATFEX [70]; <sup>c</sup> No example with the parent pyrazole, instead the 4-chloro derivative (CODBAB [40]) was used; <sup>d</sup> HESBUC [4]; <sup>e</sup> MUTKUH [59]; <sup>f</sup> No example with the parent pyrazole, instead the 4-*n*-butyl derivative (FORGIE [71]) was used.

A statistical analysis of the results in Tables 2–4 provided the following three equations:

$$\text{Averaged} = (0.98 \pm 0.01) \text{ Parent}, n = 12, R^2 = 0.998, \text{RMS residual} = 0.12 \text{ \AA} \quad (1)$$

$$\text{Averaged} = (0.96 \pm 0.01) + (0.93 \pm 0.09) \text{ dimer}, n = 20, R^2 = 0.998, \text{RMS residual} = 0.12 \text{ \AA} \quad (2)$$

$$\text{Parent} = (1.00 \pm 0.01) + (0.96 \pm 0.06) \text{ dimer}, n = 12, R^2 = 0.999, \text{RMS residual} = 0.08 \text{ \AA} \quad (3)$$

Equation (1) shows that averaged and parent pyrazole values are roughly proportional with a slope of 0.98 indicating that the averaged values are slightly smaller than the parent ones.

Equations (2) and (3) are similar, while (2) is better than (3), with a slope = 1.00 indicating that our calculated geometries that correspond to pyrazole itself are closer to a model of “parent” pyrazoles. It was found in a previous study [16] that the Ag...Ag distances of (pzAg)<sub>2</sub> are very sensitive to the ancillary ligands. If we assume that the situation is the same for the Cu(I) ligands (there are no examples of Au(I) dimers) it is sufficient to add a term (a dummy variable, one if dimers, zero if other metallacycles). The result is 0.93–0.96 Å and this indicates that the contraction of the Ag...Ag distance due to ancillary ligands is very important.

### 2.3. Energies

We start with a very simple premise that the more abundant a metallacycle of a given size found in the CSD the more stable the structure. A step further is to consider the percentages as a quantitative measurement of the stability in a sort of Maxwell-Boltzmann distribution. This implies two things: that the number of examples is very large and that the structures are in equilibrium (thermodynamic

control). Clearly these conditions are not fulfilled, but it remains interesting to explore the possibility of partial agreement. In this work we explored the ring size, in NH-pyrazole cyclamers we successfully studied the effect of the C-substituents [25,26] and, finally, in the case of Ag(I) pyrazolate dimers we studied the effect of ancillary ligands, which can have a marked effect on the Ag...Ag distance with a concomitant decrease in stability that was compensated for by the ligands [16]. Consequently, the problem is of great complexity and it is useful to remember that the mechanism of crystal growth is also complex and is not fully understood [72,73].

In an effort to compare the stabilities of the different metallacycles we calculated their relative free energies,  $\Delta G_{\text{rel}}$  in  $\text{kJ mol}^{-1}$ , per metallacycle and per monomer. The results are provided in Table 5.  $\delta\Delta G_{\text{rel}} = [\Delta G_{\text{rel}} - \Delta G_{\text{rel}}(\text{minimum})] \times n$ . The values corresponding to “true” dimers, trimers, tetramers, pentamers and hexamers are marked in bold for comparison with the percentages in Table 1. The more negative the  $\Delta G_{\text{rel}}$ , the more stable the metallacycle (the monomer is not a metallacycle) while the higher the  $\delta\Delta G_{\text{rel}}$  the less stable the metallacycle for any given  $n$ .

**Table 5.** Relative free energies per monomer,  $\Delta G_{\text{rel}}$  and  $\delta\Delta G_{\text{rel}}$ , in  $\text{kJ}\cdot\text{mol}^{-1}$ , of the metallacycles formed by the parent pyrazolate ligand and the coinage metals  $M = \text{Cu(I)}$ ,  $\text{Ag(I)}$  and  $\text{Au(I)}$ :  $(\text{pzM})_n$  for  $n = 2, 3, 4, 5$  and  $6$ .

<i>n</i> -mer	Cu(I)		Ag(I)		Au(I)		H	
	$\Delta G_{\text{rel}}$	$\delta\Delta G_{\text{rel}}$	$\Delta G_{\text{rel}}$	$\delta\Delta G_{\text{rel}}$	$\Delta G_{\text{rel}}$	$\delta\Delta G_{\text{rel}}$	$\Delta G_{\text{rel}}$	$\delta\Delta G_{\text{rel}}$
Monomer	0	-	0	-	0	-	0	-
<b>Dimer</b>	<b>-211.4</b>	<b>0.0</b>	<b>-171.6</b>	<b>0.0</b>	<b>-165.5</b>	<b>0.0</b>	<b>-3.5</b>	-
1 + 1	-149.2	124.3	-126.4	90.4	-108.0	115.0	-	-
<b>Trimer</b>	<b>-254.4</b>	-	<b>-213.0</b>	-	<b>-256.0</b>	-	<b>-4.5</b>	-
<b>Tetramer</b>	<b>-256.0</b>	<b>0.0</b>	<b>-214.2</b>	<b>0.0</b>	<b>-257.8</b>	<b>0.0</b>	<b>-5.6</b>	-
2 + 2	-235.0	84.3	-202.8	45.4	-182.4	301.6	-	-
2 + 2 twisted	-229.4	106.7	-193.2	83.6	-182.1	302.8	-	-
<b>Pentamer</b>	<b>-259.4</b>	-	<b>-218.5</b>	-	<b>-253.9</b>	-	-	-
<b>Hexamer</b>	<b>-269.3</b>	<b>31.3</b>	<b>-230.0</b>	<b>33.5</b>	<b>-269.3</b>	<b>21.6</b>	<b>-2.0</b>	<b>10.6</b>
Hexamer <i>ududud</i>	-255.4	114.6	-213.6	131.9	-257.3	93.6	-3.7	0.0
3 + 3	-274.5	0.0	-235.6	0.0	-272.9	0.0	-	-
3 + 3 twisted	-271.3	19.4	-232.2	20.0	-272.6	1.8	-	-

To compare the data in Table 1 (crystal structures) and Table 5 (free energies) it is necessary to remember that in Table 1 the “2 + 2” and “3 + 3” structures are classified as dimers and trimers not as tetramers and hexamers, thus even if there are “3 + 3” structures that are more stable than hexamers, this does not affect the order of the values in bold.

Several main conclusions can be drawn from the values reported in Table 6:

1. Experimental metallacycles: mainly trimers, then dimers and tetramers, some hexamers, no pentamers.

2. Experimental cyclamers (NH-pyrazoles): dimers, tetramers and trimers, are common; hexamers are very rare and there are no pentamers. This is not identical but reasonably similar to the trend in experimental metallacycles. Note that the differences in cyclamers are insignificant (less than  $6 \text{ kJ mol}^{-1}$ ) compared with metallacycles (Cu:  $-211.4/-269.3$ ; Ag:  $-171.6/-232.3$ ; Au:  $-165.5/-269.3 \text{ kJ mol}^{-1}$ ); this explains that steric effects of the substituents in cyclamers are sufficient to explain the size of the cycle (see point 6).

3. The absence of pentamers in the CSD can be due to the fact that pentameric species are crystallographically prohibited by “normal” rotational symmetry. Thus, perhaps more of these species exist but have not been crystallized for this reason.

4. Calculated metals: the order (in bold, Table 4) for Cu and Ag is hexamers, pentamers, tetramers, trimers and dimers; for Au the order is hexamers, tetramers, trimers, pentamers and dimers.

5. Metals: comparison of experimental vs. calculated values shows that there is no relationship between these, which means that the ring size is not the determining factor. Other factors such as steric effects of the substituents in the 3- and 5-positions, the roles of ancillary ligands, solvates and co-crystals as well as the kinetics of crystal growth could all play a determining role.

6. NH: there is a weak relationship for experimental vs. calculated values. Remember that in the experimental case the main factor is the steric effect of the substituents at the 3- and 5-positions [26].

7. There is no relationship between the order of calculated metals vs. that of calculated H.

**Table 6.** Comparison of the populations of Tables 1 and 5 (absolute values).

Metal/H	% Dimers	% Trimers	% Tetramers	% Pentamers	% Hexamers
Cu(I)	<b>2</b> [27.2]	<b>1</b> [50.6]	<b>3</b> [22.2]	<b>5</b> [0.0]	<b>4</b> [0.0]
Ag(I)	<b>2</b> [6.2]	<b>1</b> [75.0]	<b>3</b> [6.2]	<b>5</b> [0.0]	<b>4</b> [2.1]
Au(I)	<b>4</b> [0.0]	<b>1</b> [75.7]	<b>2</b> [21.6]	<b>5</b> [0.0]	<b>3</b> [2.7]
H	<b>1</b> [42.1]	<b>3</b> [21.1]	<b>2</b> [34.2]	<b>5</b> [0.0]	<b>4</b> [2.6]
	$\Delta G_{rel}$ dimers	$\Delta G_{rel}$ trimers	$\Delta G_{rel}$ tetramers	$\Delta G_{rel}$ pentamers	$\Delta G_{rel}$ hexamers
Cu(I)	<b>5</b> 211.4	<b>4</b> 254.4	<b>3</b> 256.0	<b>2</b> 259.4	<b>1</b> 269.3
Ag(I)	<b>5</b> 171.6	<b>4</b> 213.0	<b>3</b> 214.2	<b>2</b> 218.5	<b>1</b> 232.2
Au(I)	<b>5</b> 165.5	<b>3</b> 256.0	<b>2</b> 257.8	<b>4</b> 253.9	<b>1</b> 269.3
H	<b>4</b> 3.5	<b>2</b> 4.5	<b>1</b> 5.6	-	<b>3</b> 3.7 <b>5</b> 2.0

#### 2.4. QTAIM Analysis

This study was limited to Au(I) because, as explained in the introduction, it is the most interesting metal and we have published two significant papers on this topic [17,19]. The AIM analysis was also employed successfully in a related work [16].

Analysis of the electron density within the QTAIM shows the presence of bond critical points (BCPs) that link the gold atoms with the nitrogen atoms, other gold atoms, and in one case, with a carbon atom (1 + 1). The molecular graph of all of the systems is provided in Figure 20 with an indication of the position of the electron density critical points and the bond paths that link the BCPs with the nuclei. The topological description is very simple for the monomer, trimer, tetramer, and hexamer (*ududud*), in which only sequential Au-N BCPs are found linking the different systems. In the rest of the cases, an Au-Au BCP and additional Au-N BCPs are found. The Au-N BCPs (17 unique contacts) are found for interatomic distances between 1.99 and 3.68 Å. The electron density at the BCPs ranges between 0.145 and 0.006 au, thus showing in all cases positive Laplacian values (between 0.423 and 0.018 au). These results are characteristics of BCPs between atoms with very different electronegativities. The negative value of the total energy at the BCP for those contacts with interatomic distances shorter than 2.2 Å is an indication of the partial covalent character of these interactions.

The Au-Au BCPs (seven unique cases) are present for interatomic distances between 2.81 and 4.02 Å. The electron density values range between 0.042 and 0.005 au with positive Laplacian values. As observed previously, some of the BCPs present negative values for the total energy density (interatomic distances shorter than 3.4 Å).

In the two types of BCPs analyzed in this research, excellent exponential relationships ( $R^2 > 0.99$ ) were found between the electron density or the Laplacian at the BCP vs. the interatomic distance, a finding that is consistent with previous reports in the literature for other contacts [16,74–78].

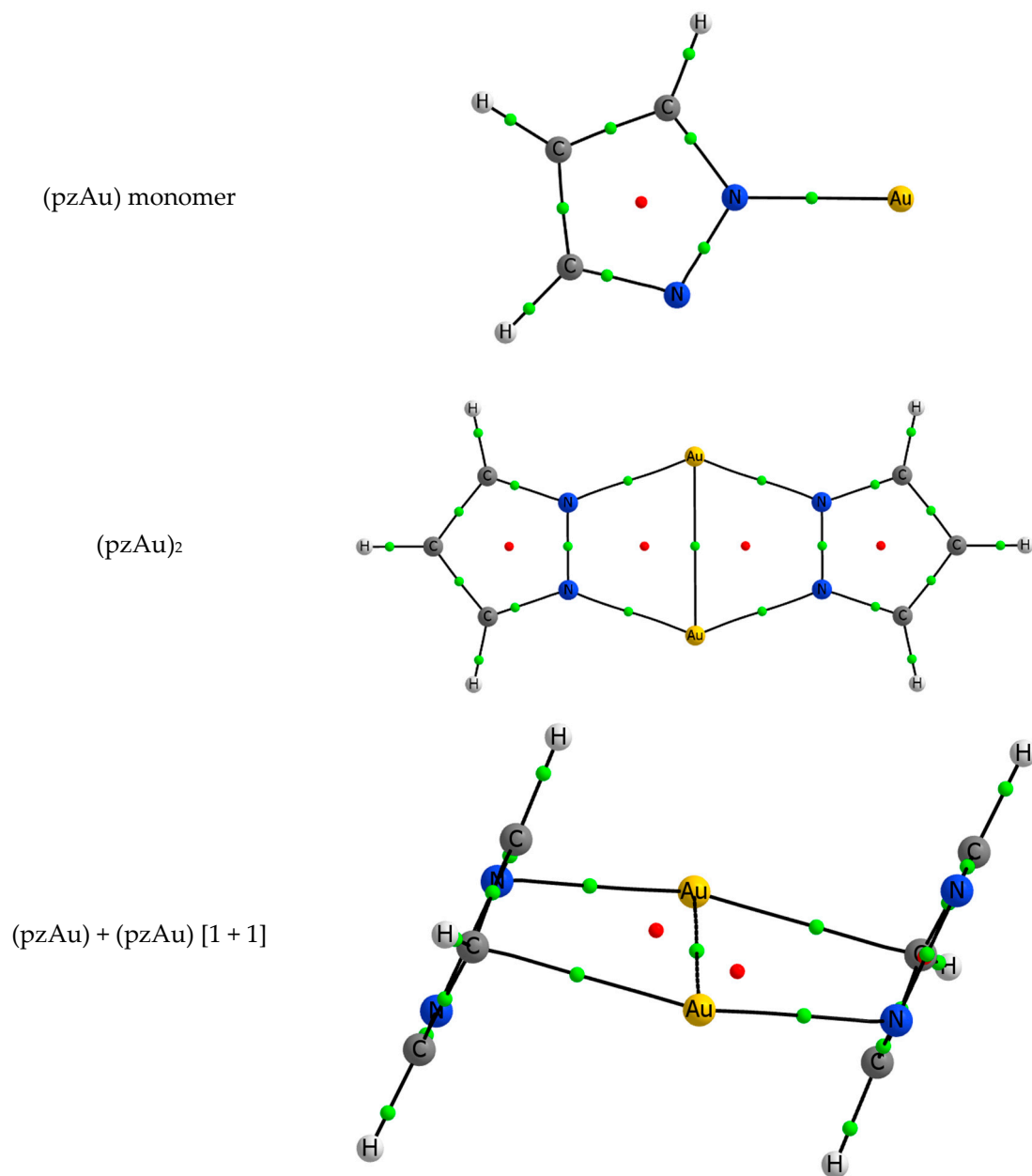


Figure 18. Cont.

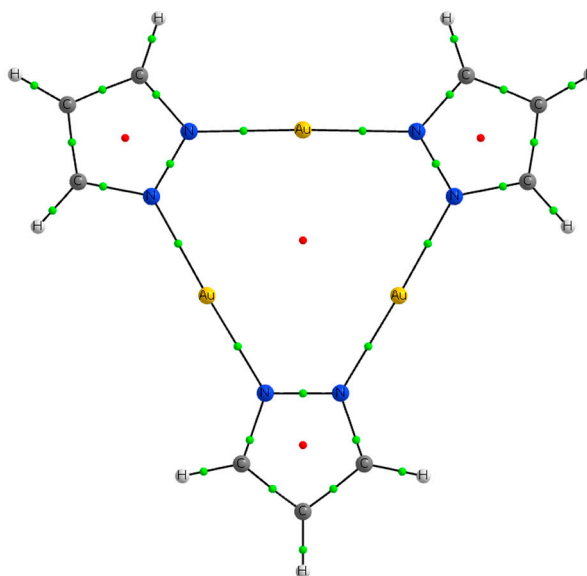
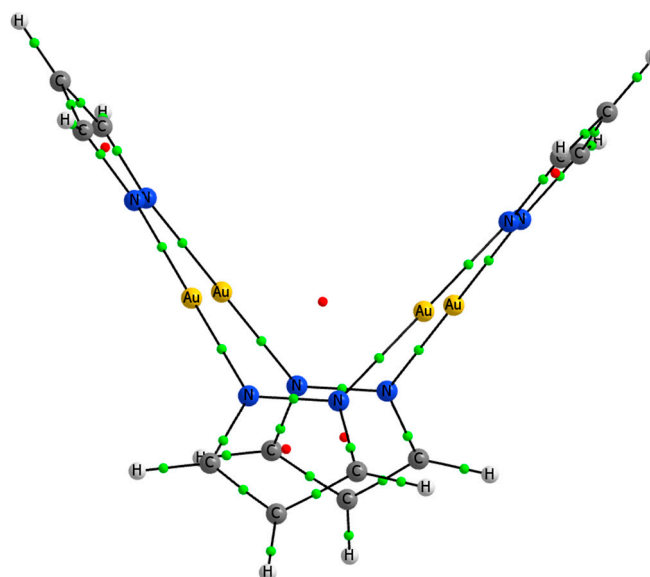
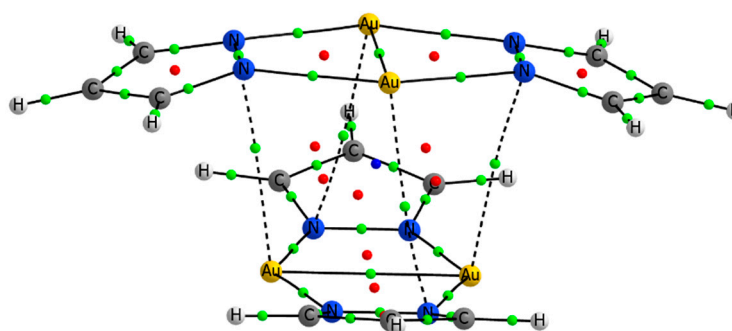
$(\text{pzAu})_3$  $(\text{pzAu})_4$  $(\text{pzAu})_2 + (\text{pzAu})_2 [2 + 2]$ 

Figure 19. Cont.

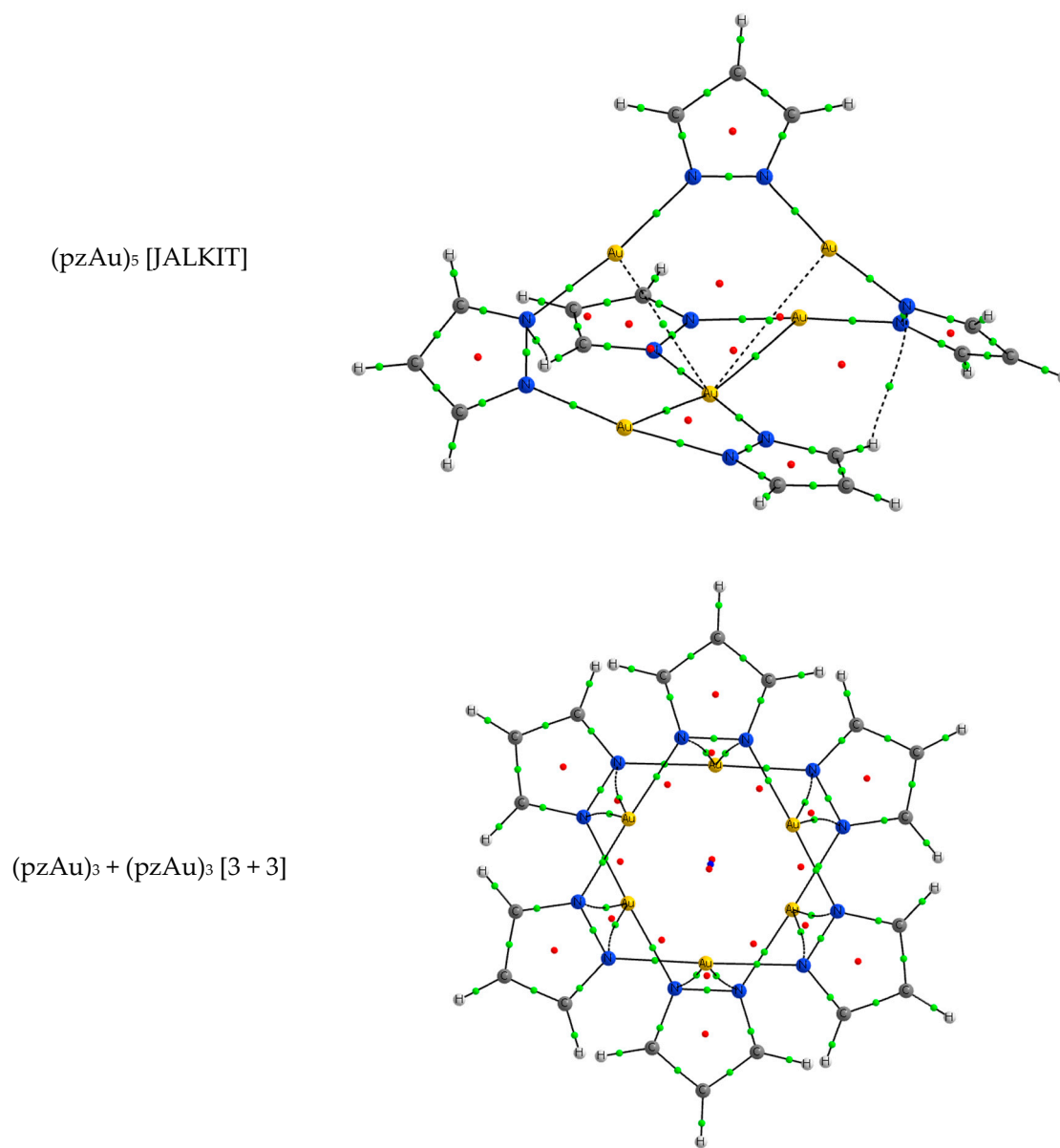
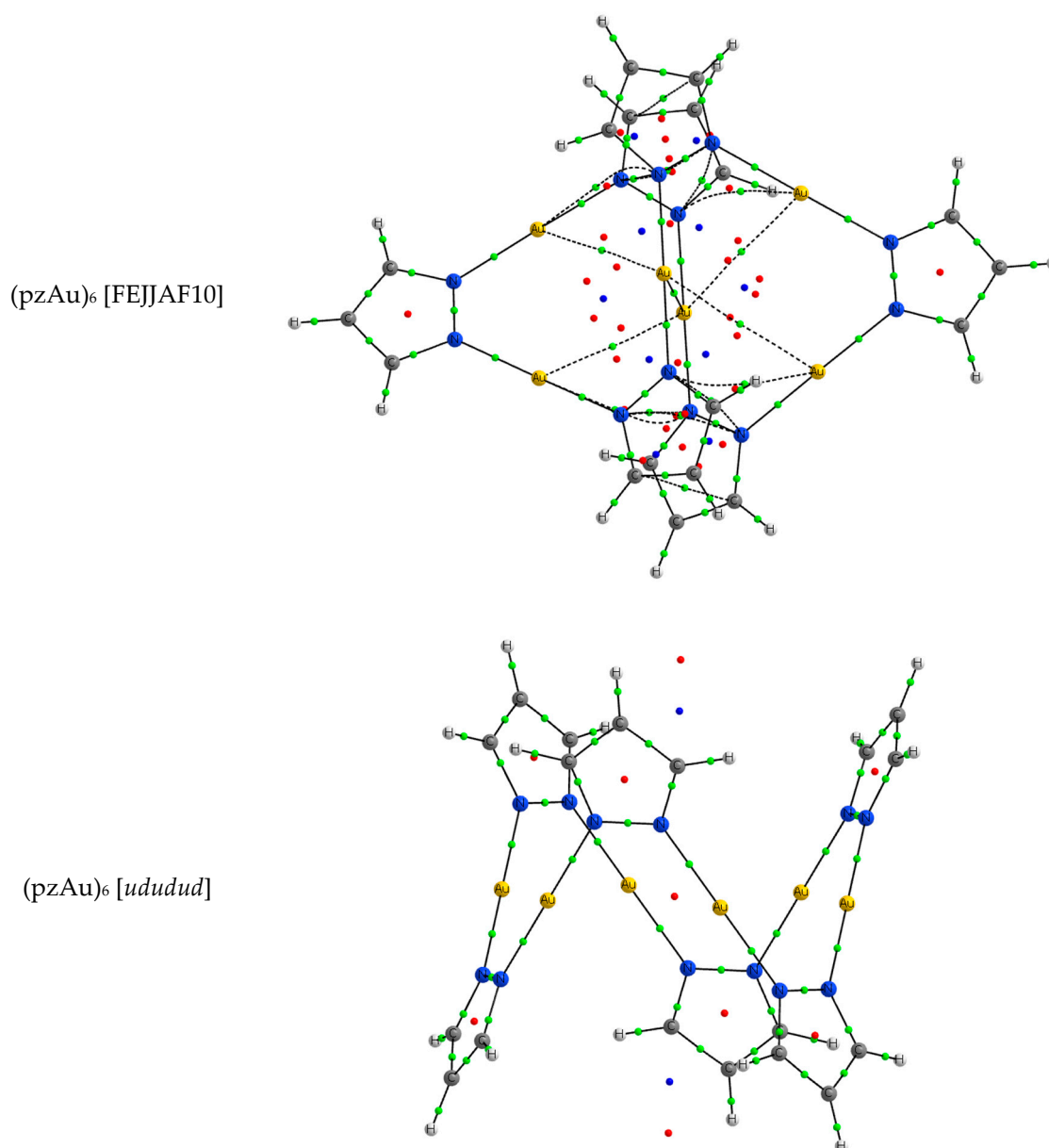


Figure 20. Cont.



**Figure 20.** Molecular graph of the (pzAu)<sub>n</sub> complexes studied. The location of the bond, ring, and cage critical points are indicated with green red and blue dots.

### 3. Methods

The crystal structures with (pzM)<sub>n</sub> systems were searched in the CSD database 5.41 (November 2019) [20]. The M06-2x DFT functional [79] in combination with the jul-cc-pVDZ basis set [80,81] for the light atoms (C, N and H) and the aug-cc-pVDZ-PP effective core potential basis set [82] for the Cu, Ag and Au atoms were used for the theoretical calculations, all of them for isolated molecules in gas phase. The geometry optimization and frequency calculations were carried out with the Gaussian-16 package [83]. In all cases, the geometries obtained correspond to energetic minima (no imaginary frequencies).

The electron density of the systems was analyzed within the quantum theory of the atoms in molecules (QTAIM) [21,23] theory with the AIMAll program [84]. This program allows location and characterization of the critical points of the electron density (nuclear attractor, bond, ring and cage critical points).



#### 4. Conclusions

The main conclusions of this work concerning the structure in the solid state of metallacycles of pyrazolates and coinage metals are:

1. The exploration of the CSD yielded a considerable number of crystal structures and this allowed a statistical analysis of the abundance of different cycles.
2. All examples contain only a single metal although it should not present any difficulties to prepare metallacycles with two or three metals.
3. Dimers and trimers are common in the case of Cu(I). Dimers in all cases contain other ligands. Double trimers (3 + 3) should not be confused with hexamers, which are not known. Pentamers are also not known. There is no reason why hexamers could not be prepared, but the main difficulty is that a method does not exist that allows selection a priori of the size of the ring.
4. Dimers and trimers are also common in the case of Ag(I). There are examples in which the hexagonal ring of dimers is planar, folded (boat-type) and folded (chain-type). In this case there are examples of “true” hexamers (no “3 + 3” double trimers), but otherwise Ag(I) and Cu(I) are similar.
5. In the case of Au(I) dimers are not known “all dimers are Au(III) derivatives”. The double trimers form different patterns that can be classified according to the triangles formed by the three Au atoms. Tetramers are frequently found.
6. Calculations on simplified models (i.e., without C-substituents or other ligands) reproduce well the geometries but not the energies found experimentally, with stability increasing with ring size.
7. AIM analysis of the gold derivatives shows the presence of several Au-N and Au-Au BCPs and in one case an Au-C BCP.

**Author Contributions:** I.A. performed the calculations and the survey of the CSD. J.E. and I.A. contributed equally to the writing of this paper. Both authors have read and agreed to the published version of the manuscript.

**Funding:** We are grateful to the Spanish MICINN for financial support through project CTQ2018-094644-B-C22 and Comunidad de Madrid (P2018/EMT-4329 AIRTEC-CM).

**Acknowledgments:** Thanks are given to the CTI (CSIC) and the Irish Centre for High-End Computing (ICHEC) for their continued computational support. The authors would like to thank one of the reviewers for the idea that pentamers are crystallographically prohibited by “normal” rotational symmetry.

**Conflicts of Interest:** The authors declare no conflict of interest.

#### References

1. Zheng, J.; Lu, Z.; Wu, K.; Ning, G.-H.; Li, D. Coinage-Metal-Based Cyclic Trinuclear Complexes with Metal-Metal Interactions: Theories to Experiments and Structures to Functions. *Chem. Rev.* **2020**, *120*, 9675–9742. [[CrossRef](#)]
2. Okkersen, H.; Groenveld, W.L.; Reedijk, J. Pyrazoles and imidazoles as ligands. Part XVIII. Neutral and anionic pyrazole coordinated to Cu(I) and Ag(I). *Rec. Trav. Chim. Pays Bas.* **1973**, *92*, 945–953. [[CrossRef](#)]
3. Minghetti, G.; Banditelli, G.; Bonati, F. Metal derivatives of azoles. 3. The pyrazolato anion (and homologues) as a mono- or bidentate ligand: Preparation and reactivity of tri-, bi, and mononuclear gold(I) derivatives. *Inorg. Chem.* **1979**, *18*, 658–663. [[CrossRef](#)]
4. Masciocchi, N.; Moret, M.; Cairati, P.; Sironi, A.; Ardizzioia, G.A.; La Monica, G. The Multiphase Nature of the Cu(pz) and Ag(pz) (Hpz = Pyrazole) Systems: Selective Syntheses and Ab-Initio X-ray Powder Diffraction Structural Characterization of Copper(I) and Silver(I) Pyrazolates. *J. Am. Chem. Soc.* **1994**, *116*, 7668–7676. [[CrossRef](#)]
5. Ghazalli, N.F.; Yuliati, L.; Lintang, H.O. Molecular Self-Assembly of Group 11 Pyrazolate Complexes as Phosphorescent Chemosensors for Detection of Benzene. *IOP Conf. Ser. Mater. Sci. Eng.* **2018**, *299*, 12029. [[CrossRef](#)]
6. Lakhi, J.S.; Patterson, M.R.; Dias, H.V.R. Coinage metal metallacycles involving a fluorinated 3,5-diarylpyrazolate. *New J. Chem.* **2020**, *44*, 14814–14822. [[CrossRef](#)]
7. Fujisawa, K.; Saotome, M.; Takeda, S.; Young, D.J. Structures and Photoluminescence of Coinage Metal(I) Phenylpyrazolato Trinuclear Complexes [M(3,5-Et2-4-Ph-pz)]<sub>3</sub> and Arene Sandwich Complexes {[Ag(3,5-Et2-4-Ph-pz)]<sub>3</sub>}<sub>2</sub>(Ar) (Ar = Mesitylene and Toluene). *Chem. Lett.* **2020**, *49*, 670–673. [[CrossRef](#)]

8. Barberá, J.; Elduque, A.; Giménez, R.; Oro, L.A.; Serrano, J.L. Pyrazolate “Golden” Rings: Trinuclear Complexes That Form Columnar Mesophases at Room Temperature. *Angew. Chem. Int. Ed.* **1996**, *35*, 2832–2835. [[CrossRef](#)]
9. Barberá, J.; Lantero, I.; Moyano, S.; Serrano, J.L.; Elduque, A.; Giménez, R. Silver pyrazolates as coordination-polymer luminiscent metallomesogens. *Chem. Eur. J.* **2010**, *16*, 14545–14553. [[CrossRef](#)] [[PubMed](#)]
10. Beltrán, E.; Barberá, J.; Serrano, J.L.; Elduque, A.; Giménez, R. Chiral Cyclic Trinuclear Gold(I) Complexes with a Helical Columnar Phase. *Eur. J. Inorg. Chem.* **2014**, *2014*, 1165–1173. [[CrossRef](#)]
11. Cored, J.; Crespo, O.; Serrano, J.L.; Elduque, A.; Giménez, R. Decisive Influence of the Metal in Multifunctional Gold, Silver, and Copper Metallacycles: High Quantum Yield Phosphorescence, Color Switching, and Liquid Crystalline Behavior. *Inorg. Chem.* **2018**, *57*, 12632–12640. [[CrossRef](#)] [[PubMed](#)]
12. Ovejero, P.; Mayoral, M.J.; Cano, M.; Lagunas, M.C. Luminescence of neutral and ionic gold(I) complexes containing pyrazole or pyrazolate-type ligands. *J. Organomet. Chem.* **2007**, *692*, 1690–1697. [[CrossRef](#)]
13. Caramori, G.F.; Piccoli, R.M.; Segala, M.; Muñoz-Castro, A.; Guajardo-Maturana, R.; Andrada, D.M.; Frenking, G. Cyclic trinuclear copper(i), silver(i), and gold(i) complexes: A theoretical insight. *Dalton Trans.* **2015**, *44*, 377–385. [[CrossRef](#)] [[PubMed](#)]
14. Alkorta, I.; Elguero, J.; Dias, H.V.R.; Parasar, D.; Martín-Pastor, M. An experimental and computational NMR study of organometallic nine-membered rings: Trinuclear silver(I) complexes of pyrazolate ligands. *Magn. Reson. Chem.* **2020**, *58*, 319–328. [[CrossRef](#)] [[PubMed](#)]
15. Fujisawa, K.; Okano, M.; Martín-Pastor, M.; López-Sánchez, R.; Elguero, J.; Alkorta, I. Multinuclear magnetic resonance studies of five silver(I) trinuclear pyrazolate complexes. *Struct. Chem.* **2020**, in press. [[CrossRef](#)]
16. Alkorta, I.; Trujillo, C.; Sánchez-Sanz, G.; Elguero, J. Regium Bonds between Silver(I) Pyrazolates Dinuclear Complexes and Lewis Bases (N<sub>2</sub>, OH<sub>2</sub>, NCH, SH<sub>2</sub>, NH<sub>3</sub>, PH<sub>3</sub>, CO and CNH). *Crystals* **2020**, *10*, 137. [[CrossRef](#)]
17. Sánchez-Sanz, G.; Trujillo, C.; Alkorta, I.; Elguero, J. Understanding Regium Bonds and their Competition with Hydrogen Bonds in Au<sub>2</sub>:HX Complexes. *ChemPhysChem* **2019**, *20*, 1572–1580. [[CrossRef](#)] [[PubMed](#)]
18. Sánchez-Sanz, G.; Trujillo, C.; Alkorta, I.; Elguero, J. Rivalry between regium and hydrogen bonds established within diatomic coinage molecules and Lewis acids/bases. *ChemPhysChem* **2020**. accepted. [[CrossRef](#)] [[PubMed](#)]
19. Trujillo, C.; Sánchez-Sanz, G.; Elguero, J.; Alkorta, I. The Lewis acidities of gold(I) and gold(III) derivatives: A theoretical study of complexes of AuCl and AuCl<sub>3</sub>. *Struct. Chem.* **2020**, *31*, 1909–1918. [[CrossRef](#)]
20. Groom, C.R.; Bruno, I.J.; Lightfoot, M.P.; Ward, S.C. The Cambridge Structural Database. *Acta Crystallogr. Sect. B Struct. Sci. Cryst. Eng. Mater.* **2016**, *72*, 171–179. [[CrossRef](#)]
21. Bader, R.F.W. *Atoms in Molecules: A Quantum Theory*; (International Series of Monographs on Chemistry, 22); Clarendon Press: Oxford, UK, 1990.
22. Bader, R.F.W. A quantum theory of molecular structure and its applications. *Chem. Rev.* **1991**, *91*, 893–928. [[CrossRef](#)]
23. Popelier, P.L.A. *Atoms in Molecules: An Introduction*, 1st ed.; Prentice Hall: Harlow, UK, 2000.
24. Matta, C.F.; Boyd, R.J. *An Introduction to the Quantum Theory of Atoms in Molecules*; Wiley: Hoboken, NJ, USA, 2007; pp. 1–34.
25. Foces-Foces, C.; Alkorta, I.; Elguero, J. Supramolecular structure of 1H-pyrazoles in the solid state: A crystallographic and ab initio study. *Acta Crystallogr. Sect. B Struct. Sci.* **2000**, *56*, 1018–1028. [[CrossRef](#)]
26. Alkorta, I.; Elguero, J.; Foces-Foces, C.; Infantes, L. Classification of hydrogen-bond motives in crystals of NH-pyrazoles: A mixed empirical and theoretical approach. *Arkivoc* **2006**, *ii*, 15–30. [[CrossRef](#)]
27. Mohamed, A.A.; Burini, A.; Fackler, J.P. Mixed-Metal Triangular Trinuclear Complexes: Dimers of Gold–Silver Mixed-Metal Complexes from Gold(I) Carbeniates and Silver(I) 3,5-Diphenylpyrazolates. *J. Am. Chem. Soc.* **2005**, *127*, 5012–5013. [[CrossRef](#)]
28. Mohamed, A.A.; Galassi, R.; Papa, F.; Burini, A.; Fackler, J.P. Gold(I) and Silver(I) Mixed-Metal Trinuclear Complexes: Dimeric Products from the Reaction of Gold(I) Carbeniates or Benzylimidazolates with Silver(I) 3,5-Diphenylpyrazolate. *Inorg. Chem.* **2006**, *45*, 7770–7776. [[CrossRef](#)] [[PubMed](#)]
29. Parasar, D.; Jayaratna, N.B.; Muñoz-Castro, A.; Conway, A.E.; Mykhaailiuk, P.K.; Dias, H.V.R. Carbonyl complexes of copper(I) stabilized by bridging fluorinated pyrazolates and halide ions. *Dalton Trans.* **2019**, *48*, 6358–6371. [[CrossRef](#)]

30. Ardizzoia, G.A.; Cenini, S.; La Monica, G.; Masciocchi, N.; Maspero, A.; Moret, M. Syntheses, Structures, and Reactivity of Polynuclear Pyrazolato Copper(I) Complexes, Including an ab-Initio XRPD Study of [Cu(dmpz)](3) (Hdmpz = 3,5-Dimethyl-4-nitropyrazole). *Inorg. Chem.* **1998**, *37*, 4284–4292. [[CrossRef](#)]
31. Ardizzoia, G.A.; Cenini, S.; La Monica, G.; Masciocchi, N.; Moret, M. Synthesis, X-ray Structure, and Catalytic Properties of the Unprecedented Tetranuclear Copper(I) Species [Cu(dppz)]<sub>4</sub> (Hdppz = 3,4-Diphenylpyrazole). *Inorg. Chem.* **1994**, *33*, 1458–1463. [[CrossRef](#)]
32. Dias, H.V.R.; Diyabalanage, H.V.K.; Eldabaja, M.G.; Elbjeirami, O.; Rawashdeh-Omary, M.A.; Omary, M.A. Brightly Phosphorescent Trinuclear Copper(I) Complexes of Pyrazolates: Substituent Effects on the Supramolecular Structure and Photophysics. *J. Am. Chem. Soc.* **2005**, *127*, 7489–7501. [[CrossRef](#)]
33. Titov, A.A.; Filippov, O.A.; Smol'yakov, A.F.; Baranova, K.F.; Titova, E.M.; Averin, A.A.; Shubina, E.S. Dinuclear CuI and AgI Pyrazolates Supported with Tertiary Phosphines: Synthesis, Structures, and Photophysical Properties. *Eur. J. Inorg. Chem.* **2019**, *2019*, 821–827. [[CrossRef](#)]
34. Galassi, R.; Simon, O.C.; Burini, A.; Tosi, G.; Conti, C.; Graiff, C.; Martins, N.M.R.; Da Silva, M.F.C.G.; Pombeiro, A.J.L.; Martins, L.M. Copper(I) and copper(II) metallacycles as catalysts for microwave assisted selective oxidation of cyclohexane. *Polyhedron* **2017**, *134*, 143–152. [[CrossRef](#)]
35. Omary, M.A.; Rawashdeh-Omary, M.A.; Diyabalanage, H.V.K.; Dias, H.V.R. Blue Phosphors of Dinuclear and Mononuclear Copper(I) and Silver(I) Complexes of 3,5-Bis(trifluoromethyl)pyrazolate and the Related Bis(pyrazolyl)borate. *Inorg. Chem.* **2003**, *42*, 8612–8614. [[CrossRef](#)] [[PubMed](#)]
36. Ardizzoia, G.A.; Beccalli, E.M.; La Monica, G.; Masciocchi, N.; Moret, M. Synthesis of poly(3,5-dicarbomethoxy pyrazolato)copper and its reactions with carbon monoxide and cyclohexyl isocyanide. Crystal structures of [Cu<sub>2</sub>(dcmpz)<sub>2</sub>(py)<sub>2</sub>(CO)] and [Cu(dcmpz)(RNC)]<sub>2</sub> (Hdcmpz = 3,5-dicarbomethoxy pyrazole, R = cyclohexyl). *Inorg. Chem.* **1992**, *31*, 2706–2711. [[CrossRef](#)]
37. Trose, M.; Nahra, F.; Poater, A.; Cordes, D.B.; Slawin, A.M.Z.; Cavallo, L.; Cazin, C.S. Investigating the Structure and Reactivity of Azolyl-Based Copper(I)-NHC Complexes: The Role of the Anionic Ligand. *ACS Catal.* **2017**, *7*, 8176–8183. [[CrossRef](#)]
38. Colombo, V.; Galli, S.; Choi, H.J.; Han, G.D.; Maspero, A.; Palmisano, G.; Masciocchi, N.; Long, J.R. High thermal and chemical stability in pyrazolate-bridged metal-organic frameworks with exposed metal sites. *Chem. Sci.* **2011**, *2*, 1311–1319. [[CrossRef](#)]
39. Mishima, A.; Fuyuhira, A.; Kumagai, H.; Kawata, S. Bis[μ-3,5-bis-(2-pyrid-yl)pyrazolato]bis-(hydrogensulfato)-dicopper(II) methanol disolvate. *Acta Crystallogr. Sect. E Struct. Rep. Online* **2011**, *67*, m1523–m1524. [[CrossRef](#)]
40. Yang, H.; Zheng, J.; Peng, S.-K.; Zhu, X.-W.; Wan, M.-Y.; Lu, W.; Li, D. A chemopalette strategy for white light by modulating monomeric and excimeric phosphorescence of a simple Cu(I) cyclic trinuclear unit. *Chem. Commun.* **2019**, *55*, 4635–4638. [[CrossRef](#)]
41. Ehlert, M.K.; Rettig, S.J.; Storr, A.; Thompson, R.C.; Trotter, J. Synthesis and X-ray crystal structure of the 3,5-dimethylpyrazolato copper(I) trimer, [Cu(pz'')]<sub>3</sub>. *Can. J. Chem.* **1990**, *68*, 1444–1449. [[CrossRef](#)]
42. Fujisawa, K.; Ishikawa, Y.; Miyashita, Y.; Okamoto, K.-I. Crystal Structure of Pyrazolato-bridged Copper(I) Polynuclear Complexes. *Chem. Lett.* **2004**, *33*, 66–67. [[CrossRef](#)]
43. Dias, H.V.R.; A Polach, S.; Wang, Z. Coinage metal complexes of 3,5-bis(trifluoromethyl)pyrazolate ligand. *J. Fluor. Chem.* **2000**, *103*, 163–169. [[CrossRef](#)]
44. Morawitz, T.; Lemer, H.W.; Bolte, M. cyclo-Tri(μ-2-3-phenyl-1H-pyrazole) tricopper(I). *Acta Crystallogr. Sect. E* **2006**, *62*, 1474–1476. [[CrossRef](#)]
45. Bertolotti, F.; Maspero, A.; Cervellino, A.; Guagliardi, A.; Masciocchi, N. Bending by Faulting: A Multiple Scale Study of Copper and Silver Nitropyrazolates. *Cryst. Growth Des.* **2014**, *14*, 2913–2922. [[CrossRef](#)]
46. Fujisawa, K.; Ishikawa, Y.; Miyashita, Y.; Okamoto, K.-I. Pyrazolate-bridged group 11 metal(I) complexes: Substituent effects on the supramolecular structures and physicochemical properties. *Inorganica Chim. Acta* **2010**, *363*, 2977–2989. [[CrossRef](#)]
47. Maspero, A.; Brenna, S.; Galli, S.; Penoni, A. Synthesis and characterization of new polynuclear copper(I) pyrazolate complexes and their catalytic activity in the cyclopropanation of olefins. *J. Organomet. Chem.* **2003**, *672*, 123–129. [[CrossRef](#)]
48. Titov, A.A.; Smol'yakov, A.F.; Rodionov, A.N.; Kosenko, I.D.; Guseva, E.A.; Zubavichus, Y.V.; Dorovatovskii, P.V.; Filippov, O.A.; Shubina, E.S. Ferrocene-containing tri- and tetranuclear cyclic copper(i) and silver(i) pyrazolates. *Russ. Chem. Bull.* **2017**, *66*, 1563–1568. [[CrossRef](#)]

49. Cañon-Mancisidor, W.; Gómez-García, C.J.; Espallargas, M.G.; Vega, A.; Spodine, E.; Venegas-Yazigi, D.; Coronado, E. Structural re-arrangement in two hexanuclear Cu(II) complexes: From a spin frustrated trigonal prism to a strongly coupled antiferromagnetic soluble ring complex with a porous tubular structure. *Chem. Sci.* **2014**, *5*, 324–332. [[CrossRef](#)]
50. Omary, M.A.; Rawashdeh-Omary, M.A.; Gonser, M.W.A.; Elbjeirami, O.; Grimes, T.; Cundari, T.R.; Diyabalanage, H.V.K.; Gamage, C.S.P.; Dias, H.V.R. Metal Effect on the Supramolecular Structure, Photophysics, and Acid–Base Character of Trinuclear Pyrazolato Coinage Metal Complexes. *Inorg. Chem.* **2005**, *44*, 8200–8210. [[CrossRef](#)]
51. Fujisawa, K. CSD Private Communication, 2016.
52. Morishima, Y.; Young, D.J.; Fujisawa, K. Structure and photoluminescence of silver(I) trinuclear halopyrazolato complexes. *Dalton Trans.* **2014**, *43*, 15915–15928. [[CrossRef](#)] [[PubMed](#)]
53. Yamada, S.; Ishida, T.; Nogami, T. Supramolecular triangular and linear arrays of metal-radical solids using pyrazolato-silver(I) motifs. *Dalton Trans.* **2004**, 898–903. [[CrossRef](#)]
54. Lv, X.-P.; Wei, D.; Yang, G. Hexameric Silver(I) Pyrazolate: Synthesis, Structure, and Isomerization. *Inorg. Chem.* **2017**, *56*, 11310–11316. [[CrossRef](#)]
55. Yang, G.; Raptis, R.G. Synthesis and crystal structure of tetrameric silver(I) 3,5-di-tert-butyl-pyrazolate. *Inorganica Chim. Acta* **2007**, *360*, 2503–2506. [[CrossRef](#)]
56. Georgiou, M.; Wöckel, S.; Konstanzer, V.; Dechert, S.; John, M.; Meyer, F. Structural Variations in Tetrasilver(I) Complexes of Pyrazolate-bridged Compartmental N-Heterocyclic Carbene Ligands. *Z. Naturforsch. B* **2009**, *64*, s1542–s1554. [[CrossRef](#)]
57. Titov, A.A.; Filippov, O.A.; Smol'yakov, A.F.; Averin, A.A.; Shubina, E.S. Synthesis, structures and luminescence of multinuclear silver(I) pyrazolate adducts with 1,10-phenanthroline derivatives. *Dalton Trans.* **2019**, *48*, 8410–8417. [[CrossRef](#)]
58. Woodall, C.H.; Fuertes, S.; Beavers, C.M.; Hatcher, L.E.; Parlett, A.; Shepherd, H.J.; Christensen, J.; Teat, S.J.; Intissar, M.; Rodrigue-Witchel, A.; et al. Tunable Trimers: Using Temperature and Pressure to Control Luminescent Emission in Gold(I) Pyrazolate-Based Trimers. *Chem. Eur. J.* **2014**, *20*, 16933–16942. [[CrossRef](#)]
59. Yang, G.; Raptis, R.G. Supramolecular assembly of trimeric gold(I) pyrazolates through aurophilic attractions. *Inorg. Chem.* **2003**, *42*, 261–263. [[CrossRef](#)]
60. Fronczek, F.R. CSD Private Communication, 2014.
61. Yang, G.; Raptis, R.G. Synthesis, structure and properties of tetrameric gold(I) 3,5-di-tert-butyl-pyrazolate. *Inorg. Chim. Acta* **2003**, *352*, 98–104. [[CrossRef](#)]
62. Murray, H.H.; Raptis, R.G.; Fackler, J.P., Jr. Syntheses and X-ray structures of group 11 pyrazole and pyrazolate complexes. X-ray crystal structures of bis(3,5-diphenyl-pyrazole)copper(II) dibromide, tris( $\mu$ -3,5-diphenylpyrazolato-*N,N'*) trisilver(I)-2-tetrahydro-furan, tris( $\mu$ -3,5-diphenylpyrazolato-*N,N'*) trigold(I), and hexakis( $\mu$ -3,5-diphenyl-pyrazolato-*N,N'*) hexagold(I). *Inorg. Chem.* **1988**, *27*, 26–33. [[CrossRef](#)]
63. Parasar, D.; Almotawa, R.M.; Jayaratna, N.B.; Ceylan, Y.S.; Cundari, T.R.; Omary, M.A.; Dias, H.V.R. Synthesis, Photophysical Properties, and Computational Analysis of Di- and Tetranuclear Alkyne Complexes of Copper(I) Supported by a Highly Fluorinated Pyrazolate. *Organometallics* **2018**, *37*, 4105–4118. [[CrossRef](#)]
64. Titov, A.A.; Smol'yakov, A.F.; Baranova, K.F.; Filippov, O.A.; Shubina, E.S. Synthesis, structures and photophysical properties of phosphorus-containing silver 3,5-bis(trifluoromethyl)pyrazolates. *Mendeleev Commun.* **2018**, *28*, 387–389. [[CrossRef](#)]
65. Yang, C. CSD Private Communication, 2019.
66. Kandel, S.; Stenger-Smith, J.; Chakraborty, I.; Raptis, R.G. Syntheses and X-ray crystal structures of a family of dinuclear silver(I)pyrazolates: Assessment of their antibacterial efficacy against *P. aeruginosa* with a soft tissue and skin infection model. *Polyhedron* **2018**, *154*, 390–397. [[CrossRef](#)]
67. Jayaratna, N.B.; Olmstead, M.M.; Kharisov, B.I.; Dias, H.V.R. Coinage Metal Pyrazolates [(3,5-(CF<sub>3</sub>)<sub>2</sub>Pz)M]<sub>3</sub> (M = Au, Ag, Cu) as Buckycatchers. *Inorg. Chem.* **2016**, *55*, 8277–8280. [[CrossRef](#)]
68. Yang, G.; Baran, P.; Martínez, A.R.; Raptis, R.G. Substituent Effects on the Supramolecular Aggregation of AgI-Pyrazolato Trimers. *Cryst. Growth Des.* **2012**, *13*, 264–269. [[CrossRef](#)]
69. Dias, H.V.R.; Gamage, C.S.P.; Keltner, J.; Diyabalanage, H.V.K.; Omari, I.; Eyobo, Y.; Dias, N.R.; Roehr, N.; McKinney, L.; Poth, T.; et al. Trinuclear Silver(I) Complexes of Fluorinated Pyrazolates. *Inorg. Chem.* **2007**, *46*, 2979–2987. [[CrossRef](#)]

70. Ardizzoia, G.A.; La Monica, G.; Maspero, A.; Moret, M.; Masciocchi, N. Silver(I) Pyrazolates. Synthesis and X-ray and (31)P-NMR Characterization of Triphenylphosphine Complexes and Their Reactivity toward Heterocumulenes. *Inorg. Chem.* **1997**, *36*, 2321–2328. [[CrossRef](#)]
71. Tian, A.-X.; Ning, Y.-L.; Ying, J.; Hou, X.; Li, T.-J.; Wang, X.-L. Three multi-nuclear clusters and one infinite chain induced by a pendant 4-butyl-1H-pyrazole ligand for modification of Keggin anions. *Dalton Trans.* **2015**, *44*, 386–394. [[CrossRef](#)]
72. Martins, M.A.P.; Salbego, P.R.S.; De Moraes, G.A.; Bender, C.R.; Zambiasi, P.J.; Orlando, T.; Pagliari, A.B.; Frizzo, C.P.; Hörner, M. Understanding the crystalline formation of triazene N-oxides and the role of halogen... $\pi$  interactions. *CrystEngComm* **2018**, *20*, 96–112. [[CrossRef](#)]
73. Copetti, J.P.P.; Salbego, P.R.S.; Orlando, T.; Rosa, J.M.L.; Fiss, G.F.; de Oliveira, J.P.G.; Vasconcellos, M.L.A.A.; Zanatta, N.; Bonacorso, H.G.; Martins, M.A.P. Substituent effects of 7-chloro-4-substituted quinolines. *CrystEngComm* **2020**, *22*, 4094–4107. [[CrossRef](#)]
74. Alkorta, I.; Solimannejad, M.; Provasi, P.; Elguero, J. Theoretical Study of Complexes and Fluoride Cation Transfer Between  $N_2F^+$  and Electron Donors. *J. Phys. Chem. A* **2007**, *111*, 7154–7161. [[CrossRef](#)]
75. Hugas, D.; Simon, S.; Duran, M. Electron Density Topological Properties are Useful to Assess the Difference Between Hydrogen and Dihydrogen Complexes. *J. Phys. Chem. A* **2007**, *111*, 4506–4512. [[CrossRef](#)]
76. Mata, I.; Alkorta, I.; Molins, E.; Espinosa, E. Universal Features of the Electron Density Distribution in Hydrogen-Bonding Regions: A Comprehensive Study Involving  $H\cdots X$  ( $X=H, C, N, O, F, S, Cl, \pi$ ) Interactions. *Chem. Eur. J.* **2010**, *16*, 2442–2452. [[CrossRef](#)] [[PubMed](#)]
77. Sánchez-Sanz, G.; Alkorta, I.; Elguero, J. Theoretical Study of Intramolecular Interactions in Peri-Substituted Naphthalenes: Chalcogen and Hydrogen Bonds. *Molecules* **2017**, *22*, 227. [[CrossRef](#)] [[PubMed](#)]
78. Alkorta, I.; Elguero, J.; Del Bene, J.E.; Mó, O.; Montero-Campillo, M.M.; Yáñez, M.; Romero, O.M. Mutual Influence of Pnictogen Bonds and Beryllium Bonds: Energies and Structures in the Spotlight. *J. Phys. Chem. A* **2020**, *124*, 5871–5878. [[CrossRef](#)]
79. Zhao, Y.; Truhlar, D.G. The M06 suite of density functionals for main group thermochemistry, thermochemical kinetics, noncovalent interactions, excited states, and transition elements: Two new functionals and systematic testing of four M06 functionals and 12 other functionals. *Theor. Chem. Accounts* **2008**, *120*, 215–241. [[CrossRef](#)]
80. Dunning, T.H. Gaussian basis sets for use in correlated molecular calculations. I. The atoms boron through neon and hydrogen. *J. Chem. Phys.* **1989**, *90*, 1007–1023. [[CrossRef](#)]
81. Papajak, E.; Zheng, J.; Xu, X.; Leverentz, H.R.; Truhlar, D.G. Perspectives on Basis Sets Beautiful: Seasonal Plantings of Diffuse Basis Functions. *J. Chem. Theory Comput.* **2011**, *7*, 3027–3034. [[CrossRef](#)]
82. Peterson, K.A.; Puzzarini, C. Systematically convergent basis sets for transition metals. II. Pseudopotential-based correlation consistent basis sets for the group 11 (Cu, Ag, Au) and 12 (Zn, Cd, Hg) elements. *Theor. Chem. Accounts* **2005**, *114*, 283–296. [[CrossRef](#)]
83. Frisch, M.J.; Trucks, G.W.; Schlegel, H.B.; Scuseria, G.E.; Robb, M.A.; Cheeseman, J.R.; Scalmani, G.; Barone, V.; Petersson, G.A.; Nakatsuji, H.; et al. *Gaussian 16 Rev. A.03*; Gaussian, Inc.: Wallingford, CT, USA, 2016.
84. Keith, T.A. *AIMAll, Version 19.10.12*; TK Gristmill Software: Overland Park, KS, USA, 2019.

**Sample Availability:** Not available.

**Publisher's Note:** MDPI stays neutral with regard to jurisdictional claims in published maps and institutional affiliations.



© 2020 by the authors. Licensee MDPI, Basel, Switzerland. This article is an open access article distributed under the terms and conditions of the Creative Commons Attribution (CC BY) license (<http://creativecommons.org/licenses/by/4.0/>).